THE METEOROLOGICAL MAGAZINE

HER MAJESTY'S STATIONERY OFFICE

November 1987

Met.O.978 No. 1384 Vol. 116

THE METEOROLOGICAL MAGAZINE

No. 1384, November 1987, Vol. 116

551.575.1:551.501.796

Observations of the structure of a deep fog

R. Brown

Meteorological Office, Bracknell

Summary

Profiles of temperature, wind, visibility and net radiation through a deep radiation fog are presented. The emergence of an elevated layer in the pattern of echoes from an acoustic sounder is related to the development of a lapse rate within the fog. Significant features of the profiles, such as an elevated maximum in wind shear, are described. The remarkable constancy of the temperature of the fog through the night is discussed but cannot be fully explained without invoking advection.

1. Introduction

Findlater (1985) has presented the results of field investigations to evaluate the use of a low stopping-speed anemometer, a commercially-available acoustic sounder and a mini radiosonde system as aids to forecasting the development and dispersal of radiation fog. The data obtained from these instruments were also used to study the structure and development of radiation fogs. Most of the observations presented were obtained since 1982, however Findlater also considered the development of a radiation fog at Cardington on 17/18 October 1977. This was based upon temperature measurements made from the captive BALTHUM balloon which was used to make routine soundings of the boundary layer. On the same night a second captive balloon was in operation at Cardington during the period 2300–0500 GMT gathering data for studies of fog and stratocumulus by the Cloud Physics Branch of the Meteorological Office. This carried a comprehensive set of instruments and made observations with a much higher spatial and temporal resolution than the BALTHUM balloon.

Regrettably the fog data obtained during these studies has not been as widely published as the stratocumulus data, the latter being given priority because of its importance for both local forecasting and climate studies. Although not new, this data still gives a uniquely-detailed picture of the structure of a mature radiation fog and some of the observations are presented here in order to amplify the description of the fog given by Findlater, especially in the vicinity of the fog top. First,the development of a wet adiabatic lapse rate is described together with the concomitant affect on the acoustic sounder record. The central portion of the paper describes significant features of profiles of the important physical parameters, emphasizing their relationship to the fog top. Finally, using information from the profile data, the near constancy in time of the fog temperature is illustrated and then discussed in relation to the energy budget.

2. The experiment

2.1 *The experimental equipment*

The balloon-borne instrumentation comprised a thermistor, pressure transducer, point visibility meter (PVM), droplet spectrometer, two net-radiometers, two humidity sensors and a Cardington turbulence probe which made high-frequency measurements of temperature and wind. Ascents were made from 20 m above the surface to up to 75 m above the fog top.

A monostatic acoustic sounder was also in operation during the experimental period (not the commercial instrument used by Findlater). Measurements of the surface energy balance were made, comprising the net radiative flux, the soil heat flux and the latent heat flux (evaporation) from a weighing lysimeter. Further details of the instrumentation may be found in Slingo *et al.* (1982) and Caughey *et al.* (1982).

2.2 *Synoptic situation and surface observations*

On 17 October 1977 a stationary anticyclone centred over Europe produced a moist south to south-easterly flow over England. Fog from the previous night had lifted by 1200 GMT into stratus which soon dispersed to produce a warm cloudless afternoon. Surface cooling commenced by 1600 GMT, and by 2000 GMT the surface-based inversion had grown to a depth of 200 m as shown by the BALTHUM ascent. An increase in wind speed in the early part of the evening possibly prevented fog formation, although the visibility declined slowly to reach 2000 m by 2000 GMT. By 2200 GMT the visibility had decreased to 500 m and around 2230 GMT the fog thickened significantly, with the observer reporting 50 m at 2300 GMT. The appearance of a dense fog followed a decrease in surface wind speed after 2100 GMT from 3 to 1 m s^{-1} and also a decrease in dew deposition measured by the lysimeter. This ties in with the suggestion by Roach *et al.* (1976) that when the wind becomes light on a radiation night, turbulent mixing virtually ceases and therefore so does drying of the air by dew deposition. Radiative cooling of the air to the colder ground continues and can eventually lead to direct condensation into the air.

At around 2245 GMT it was still possible to see the fog top beneath the tethered balloon, this places it at about 15 m above the surface. Acquisition of data from the balloon-borne instrumentation commenced at 2300 GMT and by the time of the first ascent, 10 minutes later, the fog was 120 m deep. Thereafter it grew to a maximum height of 280 m by 0340 GMT and when recording ceased at 0500 GMT the fog was still 215 m deep.

3. Development of the temperature profile

The change in the temperature structure of the boundary layer caused by the deep fog, as measured directly and as indicated by the acoustic sounder, is shown in Fig. 1. The strength of the acoustic echoes is mainly determined by temperature fluctuations on the scale of about half the wavelength of the transmitted sound (0.1 m) (Crease *et al.* 1977). Thus the strongest echoes are received from regions experiencing turbulent mixing in the presence of a large temperature gradient. The pre-fog inversion is illustrated by data from the 2000 GMT BALTHUM ascent. At the time of the first ascent of the fully-instrumented balloon (2315 GMT) the fog was already 100 m deep and the pre-fog inversion had been transformed to an isothermal profile. The irregular temperature profile between 100 and 130 m resulted from a few minutes pause in the ascent during which the local fog-top ascended another 40 m. The final transit throughout the fog top is marked on Fig. 1(a) by horizontal bars indicating a visibility of 100 m and 500 m measured by the PVM. Although the evidence presented in section 2 suggested that dense fog may have formed locally at the surface, the dramatic increase in fog depth over a 30-minute period was most likely caused by the advection of a pre-existing fog bank. The other two profiles shown

in Fig. 1(a) (0020 and 0230 GMT) illustrate the upward growth of the fog and the transition from an isothermal to a wet adiabatic lapse rate within the fog.

The transition to a wet adiabatic lapse rate produced a dramatic change in the pattern of echoes from the acoustic sounder, as shown in Figs 1(b), 1(c) and 1(d). At the start of the observational period (2245–2320 GMT) a continuous zone of echoes extended from the surface to around 200 m (Fig. 1(b)). Such a pattern is typical of the stable boundary layer, and the echo region coincides with the surface-based inversion and the region of significant wind shear as measured by the BALTHUM earlier. Before 2250 GMT the fog was too shallow to affect the structure of the inversion, however we know that by about 2315 GMT the rapid deepening of the fog locally was associated with an isothermal profile below 100 m. This transformation had little affect on the echo pattern although a slight weakening of the echo below 100 m may be discernible. One hour later (Fig. 1(c)) the echo strengths below 130 m have decreased noticeably, whilst between 170 m and 200 m they have increased, the net effect being the emergence of an elevated echo layer. (This process is partly obscured by a permanent-echo layer between 130 and 150 m caused by spurious returns from a nearby building; this is also seen on Fig. 1(d).) Since the fog top was found to be at about 150 m at 0020 GMT, it lay beneath the developing elevated echo layer. The top of this layer still coincided with the top of the pre-fog inversion. By 0200 GMT the elevated echo layer was clearly defined with few echoes being received from the body of the fog (Fig. 1(d)). At 0235 GMT the fog top was found at 215 m, within the elevated echo layer. As shown later, this relationship persisted to the end of the observational period. The environment leading to the generation of small-scale temperature fluctuations in the vicinity of the fog top is described in detail in section 4; basically this is a region where an elevated inversion coincided with enhanced wind shear and strong radiative cooling.

4. The profile data

Examples of profiles of the basic physical parameters are shown in Figs 2(a), 2(b) and 2(c). The plotted points are instantaneous values sampled at 10-second intervals. Allowance has been made for the vertical separation of the instruments on the balloon cable which totalled 8 m. The point visibility meter measures extinction coefficient (σ) and this has been plotted against height. The visibility (V) is related to the extinction coefficient by Koschmeider's formula $V = 3.0/\sigma$. Using this relationship a scale of visibility has also been included on Figs 2(a), 2(b) and 2(c). The position of the elevated echo layer has also been delineated. The profiles have many similarities and also some interesting differences, not all of which can be explained.

4.1 *Visibility*

The first interesting feature to note is that this fog did not exhibit a marked or consistent decrease of visibility with increasing height, as has been reported by others, e.g. Pinnick *et al.* (1978). Of course it is apparent to the casual observer that the density of fog exhibits small-scale fluctuations. Features such as the minimum in visibility around 100 m in Fig. 2(b) are probably indicative of such fluctuations, rather than of the mean vertical profile. However most profiles show no trend in visibility with height, or a region of increasing visibility as in Fig. 2(b). Two of the ten profiles showed a slight decrease of visibility with height and one of these is reproduced in Fig. 2(a). The visibility has also been calculated from the fog droplet size distributions, these profiles (not illustrated) show a similar trend with height to the PVM data. Visibility profiles obtained in several other fogs at Cardington were similar to those shown here. Since the profiles terminated at 20 m above the surface it is possible that a gradient in visibility existed beneath this. The observer consistently reported a greater visibility than measured by the PVM on this night but it is dangerous to read too much into this because we do not know how comparable the two estimates are.

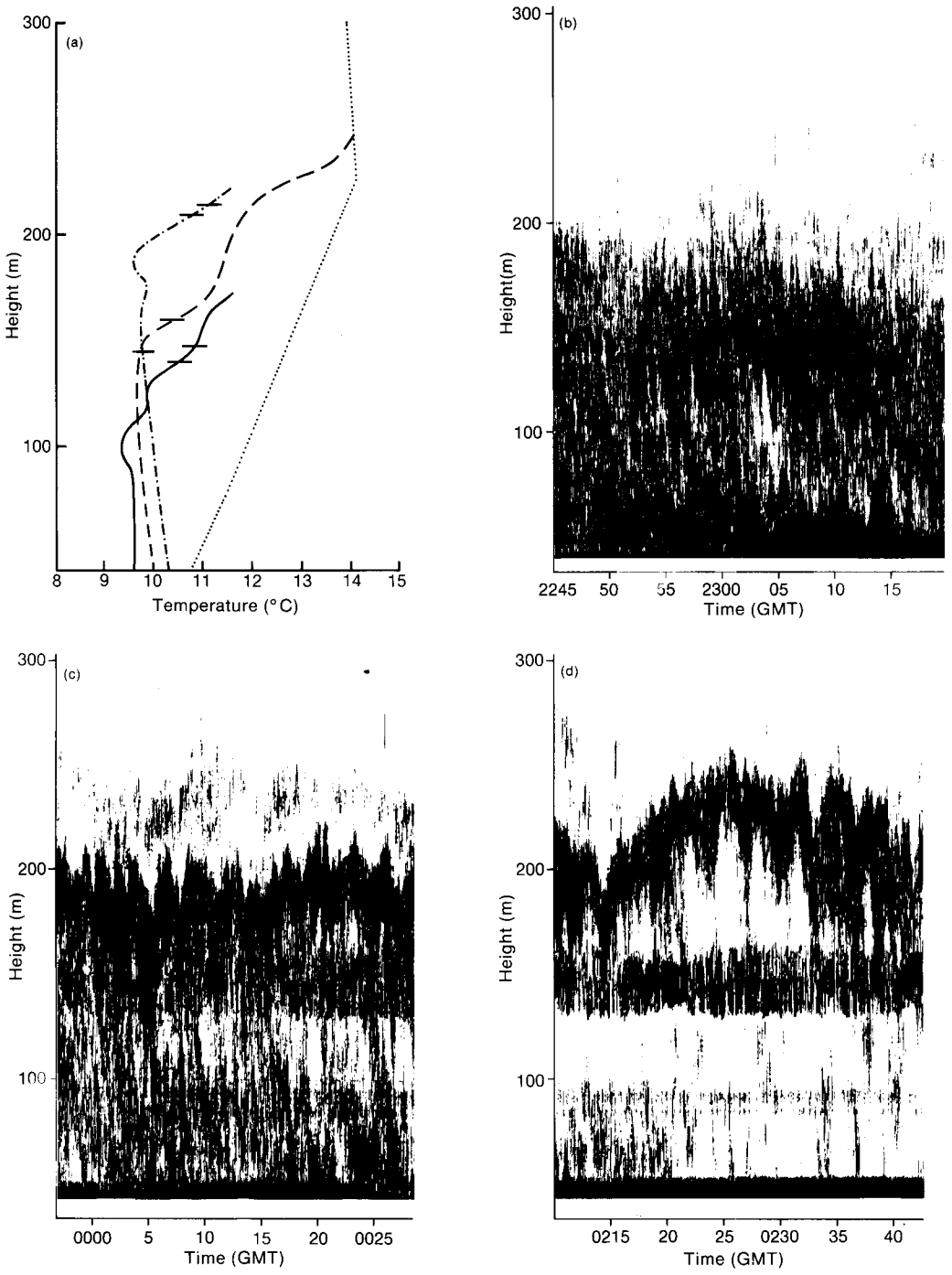

Figure 1. (a) Temperature soundings for 17/18 October 1977 at 2000 GMT(dotted line) (BALTHUM), 2315 GMT(solid line), 0020 GMT(dashed line) and 0230 GMT(dot-dash line); horizontal bars indicate visibilities of 500 m (upper bar) and 100 m (lower bar) measured by the point visibility meter. (b), (c), (d) Acoustic sounder records for the period in which the soundings in (a) were made.

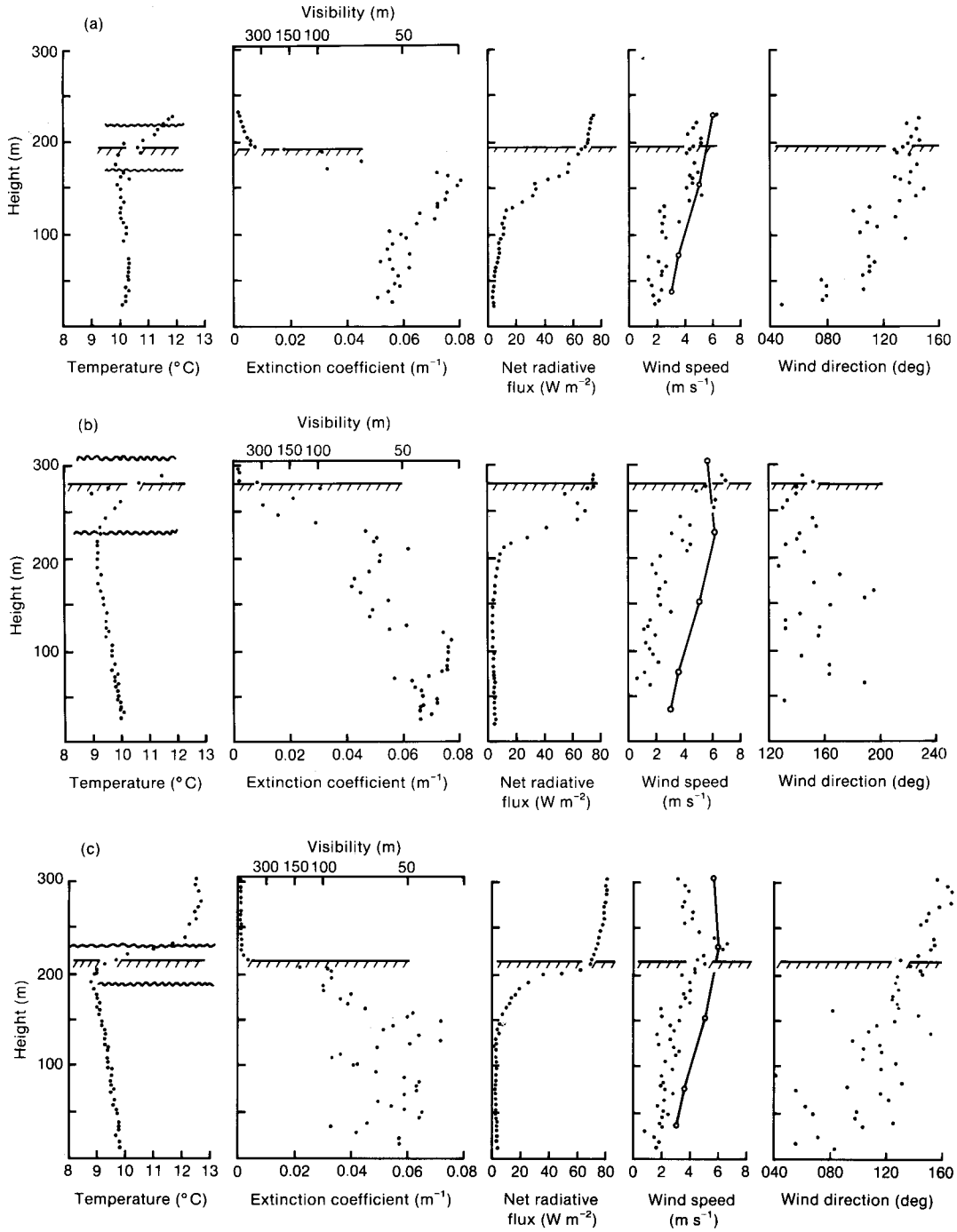

Figure 2. Profiles of temperature, extinction coefficient, net radiation and wind for (a) 0042–0047 GMT, (b) 0347–0355 GMT and (c) 0451–0500 GMT on 18 October 1977. The position of the elevated acoustic echo is marked ≈≈≈ and the fog top ////////. The wind-speed profile from the 1700 GMT BALTHUM ascent is shown as o—o .

4.2 *Fog top*

In discussing the other profiles the obvious reference point is the fog top. A complication now arises because the meteorological definition of fog, visibility less than 1000 m (extinction coefficient $>0.003\ m^{-1}$), is not relevant to the physical processes responsible for the changes in the boundary-layer temperature structure. In particular unless the visibility is less than 200–300 m the fog liquid water content will be too low to produce significant radiative cooling. Therefore in the rest of the discussion 'fog top' will refer to the top of the dense fog. This has been marked on Figs 2(a), 2(b) and 2(c) as the height where the visibility rises above 300 m (extinction coefficient falls below $0.01\ m^{-1}$).

As noted by Findlater (1985), the fog-top inversion extended into the fog. The high-resolution profiles show that sometimes the inversion base was well-defined and located close to the fog top, as in Fig. 2(c). Other profiles show the inversion merging into an isothermal layer, up to 40 m beneath the fog top, as in Fig. 2(b). On average the fog top was 25 m (standard deviation 15 m) above the inversion base. This is half the distance quoted by Findlater for the same fog. It is very likely that the difference arises from the poorer resolution of the BALTHUM ascents used by Findlater. Another factor may be the 10-minute sampling time used by the BALTHUM at every level; the fog top can fluctuate by a few tens of metres over this period. Even the continuous ascents presented here were affected by fluctuations in the fog-top height. For example the profiles illustrated in Fig. 2(b) were obtained whilst the balloon was descending. As the instruments entered the fog, the temperature fell to 9 °C and the net radiative flux also started to decrease. However at 270 m the instruments started to emerge from the fog, the temperature rose by 1 °C and the net radiative flux increased again. Either a detached patch of cold, thick fog was blown past the instruments at 280 m or the fog top descended faster than the instrument package locally.

Figs 2(a), 2(b) and 2(c) show that the elevated echo-layer coincided with the fog-top inversion and that the fog top lay within the echo layer. On average the fog top lay 25 m (standard deviation 13 m) beneath the top of the elevated echo-layer and was always contained within it. When interpreting this statistic it should be noted that the resolution of the acoustic sounder was 8 m on this occasion. (As mentioned earlier, before the emergence of the elevated echo-layer the fog top was not closely associated with the top of the echo layer.)

4.3 *Net radiative flux*

The net radiative flux profiles show that there was a net radiative loss from the fog top of about $70\ W\ m^{-2}$. The radiative cooling rate is proportional to the vertical gradient of the net radiative flux. It can be seen from Figs 2(a), 2(b) and 2(c) that the largest radiative cooling is found beneath the fog top (as defined earlier), within a layer about 70 m thick. The value is typically $3\ °C\ h^{-1}$, averaged over this layer.

A less obvious but still significant factor is the small gradient of net flux above the top of the dense fog. This indicates radiative cooling of the air above the fog to the colder fog top. The gradients in Figs 2(a) and 2(c) represent cooling rates of 0.35 and $0.55\ °C\ h^{-1}$ respectively. This cooling is analogous to the radiative cooling of the air to the colder ground which can initiate fog formation at the surface. When the relative humidity above the fog is high, radiative cooling can lead to condensation and hence the deepening of the fog.

4.4 *Wind speed and direction*

The wind speed profiles show a marked shear beneath, and sometimes through, the fog top. Inspection of all the profiles reveals a tendency for three types to occur. Sometimes there is a sharp discontinuity in wind speed a few tens of metres beneath the fog top, as in Fig. 2(a). In other profiles the shear extends over a greater depth, as in Fig. 2(b), but is still contained within the thick fog. Finally the shear can extend through the fog top, as in Fig. 2(c). This profile is atypical, however, in that it is the only

one in which the wind speed decreases markedly above the fog. Also plotted on Figs 2(a), 2(b) and 2(c) is the wind speed profile from the 1700 GMT BALTHUM (no winds are available from the 2000 GMT ascent). It can be seen that the maximum wind speed varies little through the night but relative to the 1700 GMT profile a deficit develops within the body of the fog, leading to the elevated shear-layer. The reason for this is discussed later. The wind direction was around 140° above the fog, backing to 080° towards the surface. The directional shear tended to decrease through the night, occasionally almost disappearing as in Fig. 2(b). This change cannot be explained at present. As with the wind speed some profiles show a marked change in direction a few metres beneath the fog top (e.g. Fig. 2(a)). Other profiles show a more gradual change, sometimes extending through the fog top (e.g. Fig. 2(c)). This profile also shows a marked decrease in the variability of wind direction above 160 m, which is indicative of a decrease in turbulent mixing in the capping stable-layer.

Brown (1980) has shown that a one-dimensional numerical fog model can reproduce the observed behaviour of the wind field within a mature fog. The model indicated that increased mixing within the fog (relative to the fog-free case) led to enhanced transfer of momentum to the surface. At the same time transfer of momentum from above was inhibited by the fog-top inversion. This caused a reduction in wind speed within the body of the fog (up to the top of the adiabatic region) and enhanced shear through the elevated inversion.

5. Constancy of fog temperature with time

Despite the radiative loss from the fog-top, the temperature of the fog changed little during the observational period. This is shown in more detail in Fig. 3 where the fog-top height and the temperature at several levels, including the base of the elevated inversion, have been plotted as a function of time. Unfortunately there is a gap from 0100 to 0230 GMT because of an instrument failure. From 2300 to 0100 GMT there was a rise in temperature of about 0.5 °C. The fall in temperature at 140 m was caused by the fog growing through this level between 2330 and 2350 GMT. From 0230 to 0500 GMT the temperature fell by 0.5–0.7 °C. The net result is that the temperature within the body of the fog was virtually the same at 0500 and 2300 GMT. The temperature at the inversion base fell by about 0.6 °C between these times as a result of the upward growth of the fog and the wet adiabatic lapse rate within it.

To understand this remarkable constancy of temperature we must consider the energy budget of the fog. It must be admitted at the outset that it is not possible to explain fully the observed temperature trend since advective changes appear to be important. If we consider first the cooling of a layer 200 m deep due to the observed radiative loss from the fog top and only offset by the soil heat flux (which in this case was very small, around 10 W m^{-2}), then this amounts to 0.9 °C h^{-1}. If we make the reasonable assumption that the fog-laden air is saturated, so that any cooling leads to further condensation and the release of latent heat, then the cooling rate is reduced to just under 0.4 °C h^{-1}. This is still much larger than observed, implying a cooling of 2.5 °C between 2300 and 0500 GMT.

An important factor is missing from this calculation. As the fog grows upwards, warm air from above the fog is incorporated into the body of the fog. Therefore part of the radiative cooling must be utilized in cooling this air to the temperature of the fog. In terms of the energy budget, the mixing of warm air into the fog can be represented as a downward heat flux through the fog top. The magnitude of this depends upon the temperature difference between the fog and the air above and also how fast the fog grows upwards (assuming negligible subsidence). This suggests that in order for the fog temperature to remain constant or increase it must continue to grow upwards, once growth ceases cooling should commence, which will be observed locally if advective effects are negligible. There is some support for this in Fig. 3, although cooling appears to set in before 0400 GMT whilst the fog is still deepening locally. If we assume that the fog grows upwards at 30 m h^{-1} (the mean local rate between 2330 and 0330 GMT) and the fog-top temperature difference is 2 °C, then the fog would cool at between 0.14 and 0.25 °C h^{-1}. The

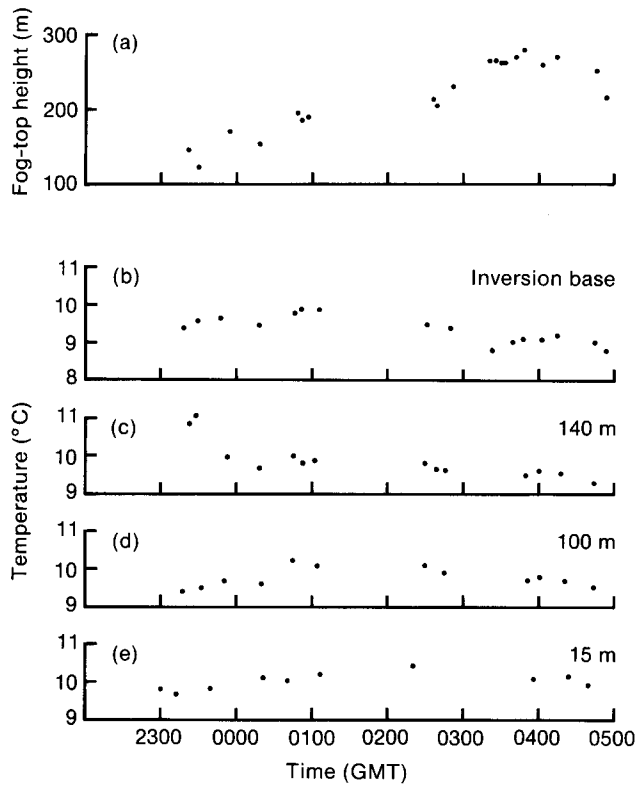

Figure 3. (a) Fog-top height as a function of time. Temperature as a function of time at (b) the inversion base, (c) 140 m, (d) 100 m and (e) 15 m above ground level.

range of values arises from the uncertainty in the measurement of the fog-top step in humidity mixing ratio. Thus the local rate of growth cannot account for the observed temperature rise until 0130 GMT and one must invoke warm advection to explain the difference. Assuming a wind speed of 4 m s^{-1} a temperature gradient of about 3 °C 100 km^{-1} would be required. There is no indication of a gradient of this magnitude from the synoptic reports upwind and downwind of Cardington, and to resolve the discrepancy further would require detailed ascents to have been made at another one or more stations.

6. Conclusions

The structure of the mature fog is best summarized by dividing the temperature profile into three regions as shown in Fig. 4.

Region A : The portion of the inversion above the top of the dense fog. Radiative cooling to the cold fog-top can lead to condensation here and hence the upward growth of the fog. The base of this region is also a source of strong acoustic-sounder echoes.

Region B : The portion of the inversion containing the dense fog. The radiative cooling rate was several degrees per hour here, yet locally the temperature changed little. Factors which can have offset the cooling include the mixing in of warmer air from above the fog, release of latent heat, and weak convective transport of heat from below. Bennetts *et al.* (1986) have described a similar situation at the top of nocturnal stratocumulus. There the radiatively-cooled air at the cloud top descends as cold downdraughts, entraining

warmer air from above the cloud and also inducing compensating warm updraughts. However, there is a difficulty in applying this picture to explain the constancy of the fog-top temperature. Within stratocumulus the adiabatic layer (region C) extends close to the cloud top with the inversion laying mainly above the cloud. However, the definition of region B reflects the fact that the inversion extends tens of metres into the fog. It is difficult to understand how radiatively-cooled air can sink through this environment. It seems likely that transport is effected by small-scale turbulence generated by the wind shear which is most pronounced within this region. This would also generate the temperature fluctuations necessary to produce the strong acoustic echoes observed from region B.

Region C : A well-mixed region as a result of weak convection generated by warming at the surface and radiative cooling at the top. The latter results from the fact that significant radiative cooling often extended beneath region B. The absence of acoustic sounder echoes from much of this region indicates negligible small-scale temperature fluctuations, despite the convection. Ascending and descending air parcels tend to follow a wet adiabat and so deviate little from the 'local' temperature. In other radiation fogs well-marked acoustic echoes, associated with convective plumes, have been observed to extend upwards from the surface (e.g. Plate III, Crease *et al.* 1977). However on this night the soil heat flux and hence the surface warming were atypically low. Occasionally, weak surface-based echoes can be seen (e.g. Fig. 1(d)) around 0215 GMT.

Although we now have some understanding of the evolution of the above structure (see for example Fig. 1, Findlater 1985), the method by which the fog grows upwards is not fully understood, nor the factors which limit the depth to which a fog can grow. For example, upward growth could be halted if the fog encountered a very dry layer. Although the humidity measurements were of poor quality in this case, there was no evidence of a very dry layer above the fog as generally encountered above stratocumulus, and the relative humidity within 50 m of the fog top probably exceeded 95%. In the numerical model referenced earlier (Brown 1980), upward growth of the fog is mainly caused by radiative cooling in region A leading to condensation. However, the model consistently underestimates

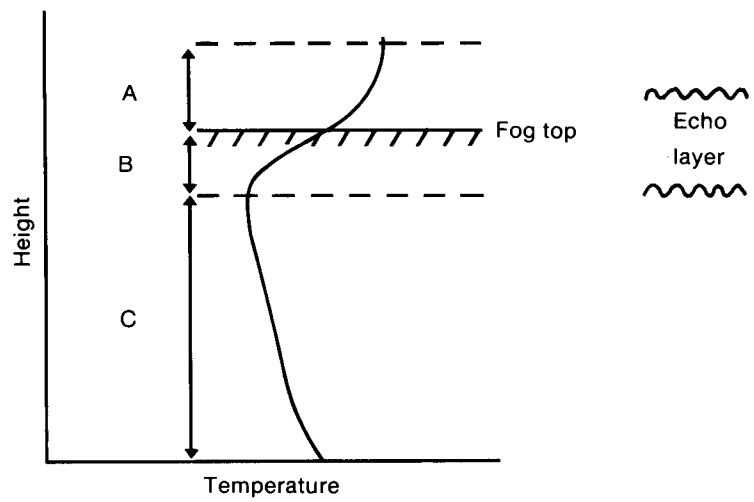

Figure 4. Idealized model of the structure of the fog.

the growth rate, for example in simulations of this case the model took 6 hours to grow the fog to a depth of 80 m. This suggests that turbulent mixing also plays an important role in the upward growth (which the model appears to underestimate).

It is possible to envisage a feedback mechanism whereby turbulence could be maintained through the fog-top inversion by the elevated maximum in wind shear. Suppose the turbulence in regions A and B decayed because the effect of stability predominated. Without the mixing in of warm air from above the fog or transport from beneath, region B would be cooled radiatively and hence region C would start to grow closer to the fog top. Upward growth of the fog would also be slowed by the cessation of turbulence. Hence the temperature gradient and wind shear aloft would tend to increase, since the changes in temperature and wind would occur over a smaller vertical distance. The flow will become turbulent again when the Richardson Number (Ri) falls below a critical value. Ri may be written in its gradient form as

$$Ri = \frac{g}{\theta} \frac{\Delta\theta \, \Delta z}{(\Delta V)^2} \qquad \ldots \ldots \ldots \ldots \ldots \ldots \quad (1)$$

where g is the acceleration due to gravity, θ the potential temperature and $\Delta\theta$, ΔV the differences in potential temperature and wind across layer depth Δz. Equation (1) shows that if the differences in temperature and wind remain constant but Δz decreases, then Ri decreases. Once it falls below a critical value turbulence will ensue, enhancing the upward growth of the fog and increasing Δz again. It is also likely that the presence of gravity waves in the stable layer (a probable cause of the undulating nature of the elevated echo layer) will result in the shear being enhanced periodically. Further measurements are required to confirm these suggestions.

Acknowledgements

The author wishes to express thanks to Dr S.J. Caughey for providing the acoustic sounder record and to Mr J. Turton for the model results. Thanks are also due to all those members of the Cloud Physics and Boundary Layer Branches of the Meteorological Office who developed the instrument package and participated in the field experiment.

References

Bennetts, D.A., McCallum, E., Nicholls, S. and Grant, J.R. 1986 Stratocumulus: an introductory account. *Meteorol Mag*, **115**, 65–76.

Brown, R. 1980 Some field observations of radiation fog and their interpretation. *In* Communications à la VIIIème conférence internationale sur la physique des nuages, Clermont-Ferrand, 15–19 juillet 1980, Vol. II. Clermont-Ferrand, UGGI.

Caughey, S.J., Crease, B.A. and Roach, W.T. 1982 A field study of nocturnal stratocumulus. II. Turbulence structure and entrainment. *Q J R Meteorol Soc*, **108**, 125–144.

Crease, B.A., Caughey, S.J. and Tribble, D.T. 1977 Information on the thermal structure of the atmospheric boundary layer from acoustic sounding. *Meteorol Mag*, **106**, 42–52.

Findlater, J. 1985 Field investigations of radiation fog formation at outstations. *Meteorol Mag*, **114**, 187–201.

Pinnick, R.G., Hoihjelle, D.L., Fernandez, G., Stenmark, E.B., Lindberg, J.D. and Hoidale, G.B. 1978 Vertical structure in atmospheric fog and haze and its effects on visible and infrared extinction. *J Atmos Sci*, **35**, 2020–2032.

Roach, W.T., Brown, R., Caughey, S.J.,Garland, J.A. and Readings, C.J. 1976 The physics of radiation fog: I — a field study. *Q J R Meteorol Soc*, **102**, 313–333.

Slingo, A., Brown, R. and Wrench, C.L. 1982 A field study of nocturnal stratocumulus; III. High resolution radiative and microphysical observations. *Q J R Meteorol Soc*, **108**, 145–165.

551.515.1:551.507.362.2

The development of an extraordinary depression — a satellite perspective

J.N. Ricketts

Meteorological Office, Bracknell

Summary

Data from the Advanced Very High Resolution Radiometer (AVHRR) on the American TIROS-N series of spacecraft provide high-resolution imagery of cloud tops and the earth's surface. Considerable detail can be observed in an AVHRR picture, but a further dimension is given to the study of atmospheric developments by the examination of a series of pictures. This article describes the evolution of cloud systems associated with the development of the deepest extra-tropical Atlantic depression ever recorded. The work took advantage of the availability of four daily passes over the area, from the combination of NOAA-9 and NOAA-10 satellites in orbit. Movie-loops of Meteosat images were also used to study the movement of cloud within the associated fronts as they crossed the British Isles.

1. Introduction

The period from late afternoon on 13 December to midnight on 15 December 1986 saw the generation of the deepest depression analysed over the North Atlantic (Burt 1987). This rapid development was followed by equally rapid decay over the next 24 hours. The depression originated from the merging of two lows; one started as a wave and was centred about 300 n mile south-south-east of Newfoundland at 1800 GMT on 13 December, while the other was a small low situated about 600 n mile to the north-east of the wave. The wave moved north-eastwards at an average speed of 75 kn over the next 12 hours, merging with the other low during the morning of the 14th. The central surface pressure of the wave fell 30 mb in the 12 hours to 0600 GMT on 14 December, followed by explosive development with a fall of 26 mb over the next 6 hours. The lowest analysed surface pressure was 916 mb at 60° N, 35° W on the midnight chart of 15 December.

Satellites are uniquely situated to provide an overall view of such developments (Schwalb 1978). NOAA-10 had been launched in September 1986 so, with NOAA-9, there are now two polar-orbiting satellites from which four Advanced Very High Resolution Radiometer (AVHRR) images can be taken each day. It was decided to make a detailed study of a series of these images so that important features might be revealed which may be common to similar such intense developments.

2. Image processing

The Satellite Meteorology Branch of the Meteorological Office uses the HERMES system (Turner *et al.* 1985) to convert raw data from meteorological satellites into useful imagery. A processed image can then be examined to identify features of a weather system, such as size, shape or cloud-top temperatures. An image is made up of pixels, rather like the dots which go to make up a newspaper photograph. Each pixel can have any one of 256 possible colours, normally represented by grey shades between white and black. In the case of an image from an infra-red sensor, this represents 256 possible temperature values. It is customary to select the colours such that the lowest temperature appears white and the highest black.

The HERMES system is capable of replacing the black and white shading with a range of colours. This is sometimes quite pretty to look at, but is of limited use. A better technique is selective colour enhancement. This involves replacing specified ranges of grey shading by a selected colour, while the other ranges stay unchanged. The colours are made up of combinations of the primaries red, green and blue. Figs 1 to 8 are pictures taken during passes over the centre of the depression throughout most of its

lifetime by NOAA-9 and NOAA-10 satellites. The palette chosen for the colour enhancement was designed both for its appearance (white, coldest; purple, warmer) and for good contrast between neighbouring colours. Each picture was calibrated automatically such that 203 K (−70 °C) was white and 303 K (+30 °C) was black, giving approximately 0.4 K between each grey shade. The temperature ranges of the colours are shown in Table I. All temperatures are calculated from measurements of the radiation emitted by the earth's surface and by cloud tops. However, water vapour absorbs radiation, thereby affecting the apparent temperature of the earth's surface and low-level clouds. These temperatures may be in error by several degrees, particularly in the tropics. At high levels, there is little water vapour outside cloud, hence satellite measurements of cloud-top temperatures at these levels are quite accurate.

Table I. *Upper and lower temperature limits (°C) of colour ranges*

Limit	White	Blue	Yellow	Green	Purple	Grey
Upper	−61.0	−53.2	−44.9	−37.9	−29.3	+30.0
Lower	−70.0	−60.6	−52.8	−44.6	−37.5	−28.9

3. The sequence of satellite pictures

The main features found in each satellite picture will now be considered (note that the times given for each picture are only approximate, due to the movement of the satellite).

In Fig. 1 there appears to be two main cloud systems; a fairly thick mass in the south, associated with the frontal wave, and an area with lower tops to the north exhibiting a hook shape which partially surrounds the centre of the more northerly depression.

By the morning of 14 December, although it appears from surface charts that the two lows have almost merged, Fig. 2 shows that the two cloud systems remain separate. The more northerly has developed extensively and has thickened into a large cloud-shield with a definite edge on the cold-air boundary. The hook feature has become detached and is now a relatively insignificant cloud area south of Cape Farewell. The more southerly cloud area, which was associated with the frontal wave, has changed little in size, although temperature values indicate that the cloud tops are at a lower height than in the previous picture. The surface centre of the wave has also become separated from the frontal cloud area.

In Fig. 3 the two cloud areas still retain their separate identify and both are now developing vigorously, each with a large shield of high-level cloud, though the cloud areas are still relatively compact in shape. The more northerly cloud mass is showing the appearance of an occlusion. The cold front associated with the more southerly cloud mass appears very weak with the higher-level cloud having moved ahead of the surface front, particularly near the triple point.

Further development of the two cloud masses has taken place by the time of the photograph shown in Fig. 4. The speckled appearance within the occlusion over south-west Iceland is of interest, perhaps indicating embedded deep convection within the frontal cloud. This may be contrasted with the more uniform appearance of the thick cloud area approaching Ireland. The surface occlusion and cold front are situated near the rear edge of the lower-level cloud-band which curves north then north-westerly from 55° N, 24° W. The two cloud masses have separated at higher levels since the previous pass, with only a narrow link remaining well ahead of the triple point.

In Fig. 5 there is continued development in the area of cloud crossing the British Isles. The occlusion has expanded in size with development now occurring preferentially to the north-west of the vortex. The surface fronts around the triple point appear to have nearly caught up with the main cloud area, while a

tongue of high cloud has moved northwards. Ahead of the cold front, three distinct levels of cloud are evident at increasing heights moving away from the front. Cold air is becoming drawn into the vortex, and convective cloud to the south is showing higher tops, implying increasing depth of cold air. The central surface-pressure of the low is approaching its minimum.

In Fig. 6 the depression is now past its maximum development. There is a large area of very cold cloud near the tip of the occlusion, over and to the west of Greenland. The vortex is becoming separated from the main cloud mass and is composed of quite-thin low- and medium-level cloud with some associated convection.

Less than five hours have passed since the last image was taken, but in Fig. 7 the appearance of the system is already less organized. Much of the frontal cloud is becoming broken, with the edge more ragged and higher-level cloud dissipating, apart from the large area around Greenland. The swirl of the vortex is less compact and the cloud more convective as cold air becomes absorbed. Deep, convective cloud has swept round the depression and is showing signs of greater concentration west of the British Isles.

Although the surface pressure at the centre of the low is still about 941 mb, the well-broken and disorganized cloud pattern shown in Fig. 8 indicates a system in an advanced state of decay. Higher-level cloud is patchy and dissipating, and the vortex is now more or less composed of convective elements. Convection in the cold air has become further concentrated showing the development of troughs with cumulonimbus activity. The 'wave' shapes in the cloud edge north of Iceland indicate minor ripples in the occlusion where baroclinic instability may be enhanced.

4. Synoptic developments

Conventional analyses of surface pressure, 500 mb and 250 mb contours and 1000–500 mb thickness contours were examined in an attempt to relate them to features on each image. Chart and image times are not coincident and interpolation is difficult, in particular because movement and development of the depression were so rapid.

At midnight on 14 December there was an intense thermal gradient between very cold air north of Newfoundland and warm air over the Atlantic to the south-east. During the following 12 hours there was an intense drive of cold air south-eastwards behind the depression and marked warm advection to the north-east ahead of it. The strong thermal advection was, perhaps, accentuated by there being two systems which extended the northerly and southerly flows at low levels before they merged. The 500 mb pattern at midnight on 14 December showed a trough with its axis extending approximately southwards across Newfoundland. This accelerated, though it did not intensify, and by midday was situated immediately behind the occlusion. At 250 mb, there was a broad flow in excess of 100 kn. The jet stream was unusually strong (about 200 kn) but the depression only reached the left exit region, favourable for cyclonic development, at about midday on 14 December, by which time considerable development had already taken place. The strongest winds passed through the cloud shields, so the definite edges do not mark the location of a jet stream, as might be expected. Instead, they probably indicate mass descent on the edges of areas of powerful ascent. It seems that the initial impetus for development of the system was thermodynamic. As the morning of 14 December progressed, the effect of dynamic influences increased and became predominant in maintaining the deepening of the system during the afternoon.

5. Conveyor belts associated with the developing system

The image taken at 0558 GMT on 14 December (Fig. 2) was timed close to a main synoptic hour, which allowed comparison of synoptic and image features. The surface analysis was available for this time and 500 mb and 250 mb patterns could be interpolated from the 0000 GMT and 1200 GMT

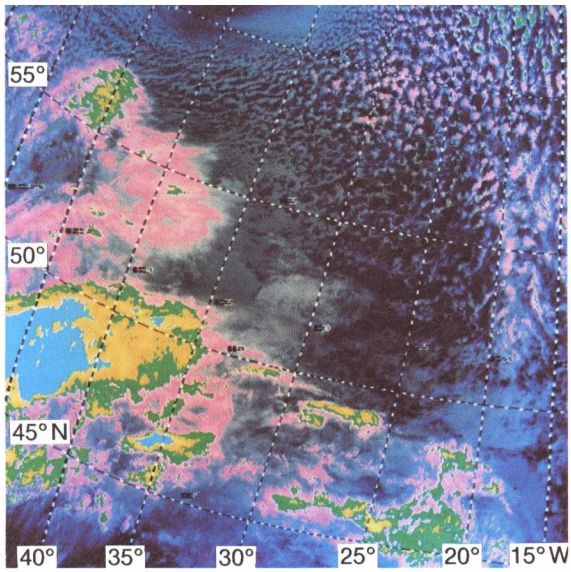

Figure 1. NOAA-10 infra-red image at 2046 GMT on 13 December 1986.

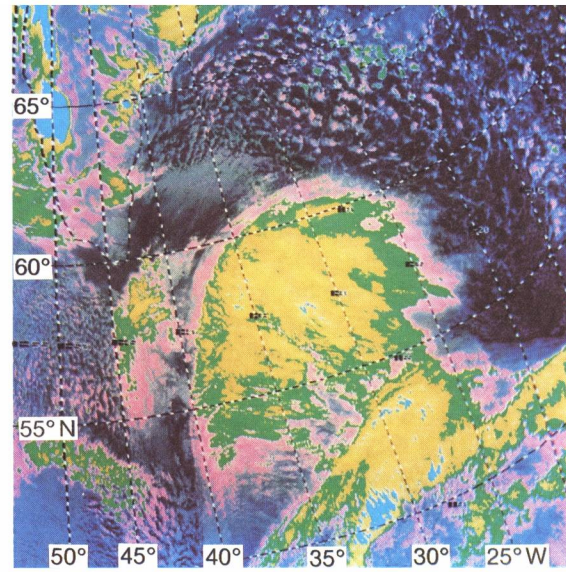

Figure 2. NOAA-9 infra-red image at 0558 GMT on 14 December 1986.

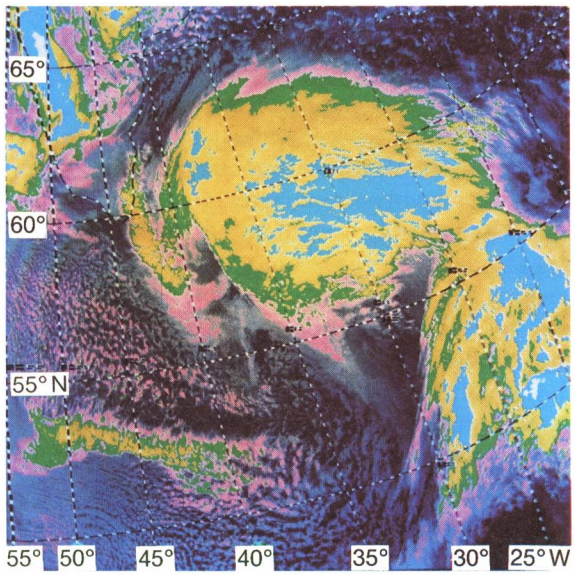

Figure 3. NOAA-10 infra-red image at 1036 GMT on 14 December 1986.

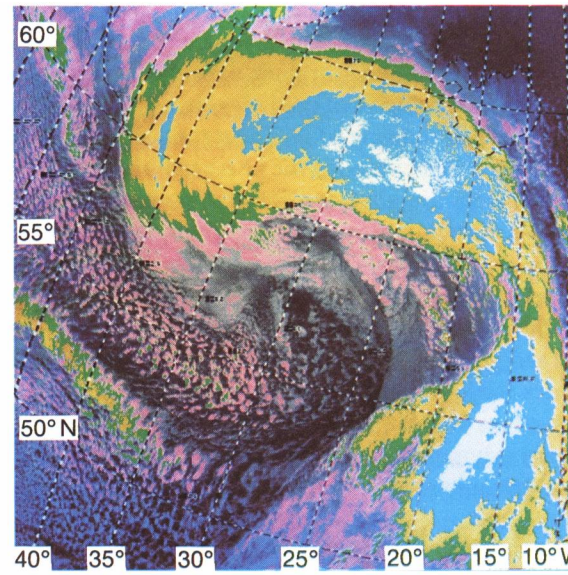

Figure 4. NOAA-9 infra-red image at 1554 GMT on 14 December 1986.

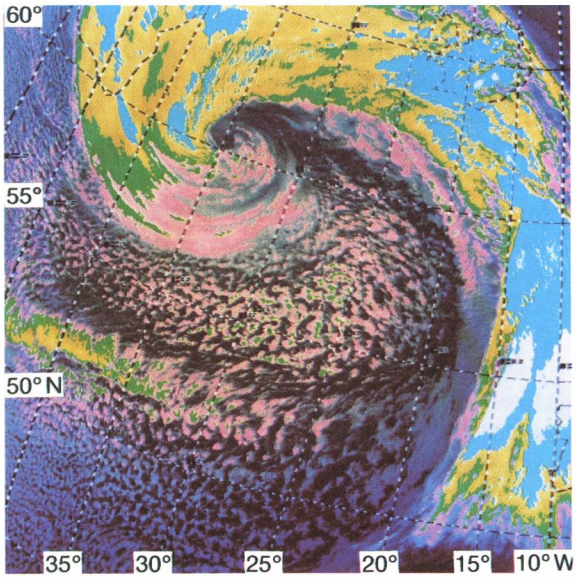

Figure 5. NOAA-10 infra-red image at 2025 GMT on 14 December 1986.

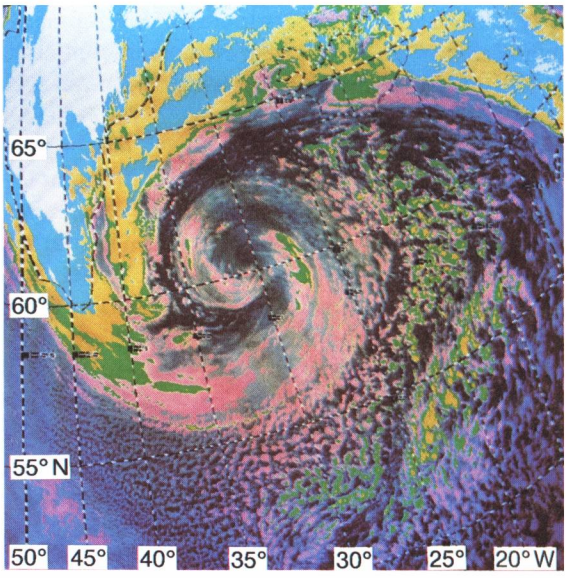

Figure 6. NOAA-9 infra-red image at 0547 GMT on 15 December 1986.

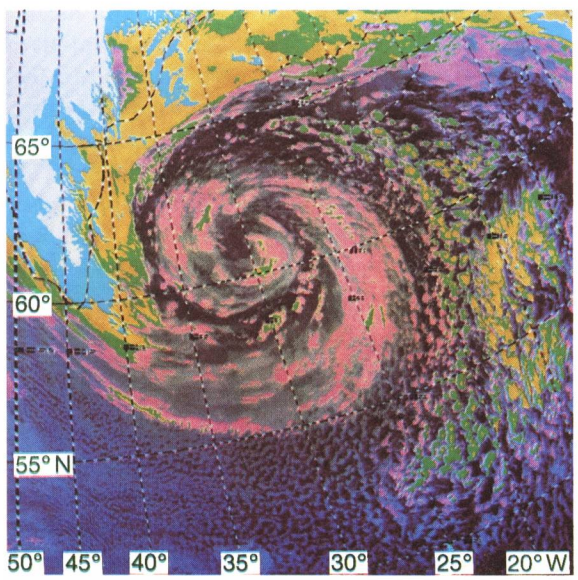

Figure 7. NOAA-10 infra-red image at 1013 GMT on 15 December 1986.

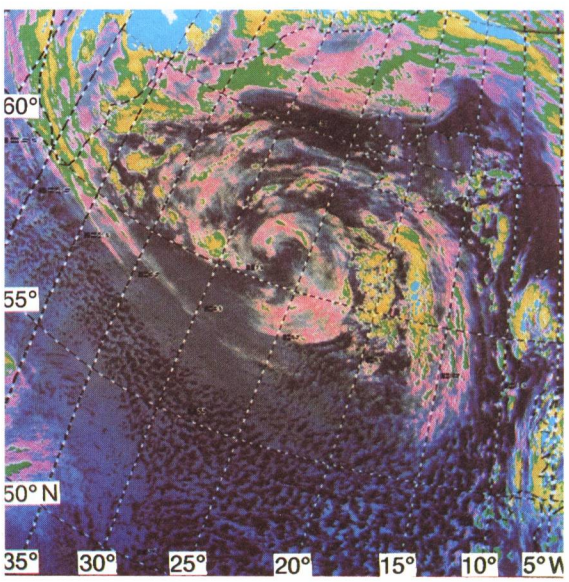

Figure 8. NOAA-10 infra-red image at 2005 GMT on 15 December 1986.

analyses. At this time, considerable development was taking place and estimations were made of the relative flows within the depression and compared with the image to see how they appeared.

The three-dimensional flow within a frontal system has been described by Browning (1985) using the concept of conveyor belts (Harrold 1973) as a means of transporting heat and moisture between different levels. The direction and velocity of the depression at this time was calculated as 200° 65 kn. The assessments of the relative flow at different levels around the depression produced the pattern as in Fig. 9, which includes an outline of the cloud distribution. It shows an ascending conveyor belt across and to the south of the triple point, turning southwards as it reaches the forward cloud edge. The picture shows that there may be two or more parallel conveyors, each ascending into the more southerly cloud area. Ahead of the warm front and occlusion, there is a low-level conveyor belt moving in towards the system, then quickly turning north as it ascends into the more northerly cloud shield. The ribbon of cloud at the rear of the system indicates a descending conveyor moving southwards towards the cold front. As the depression turned towards the north and slowed down during the day, the direction of the descending conveyor belt to the rear of the centre became closer to the ground-relative flow pattern. The diffuse nature of the forward edge of the cloud masses is consistent with marked descent ahead of the system, where the relative motions turn southwards.

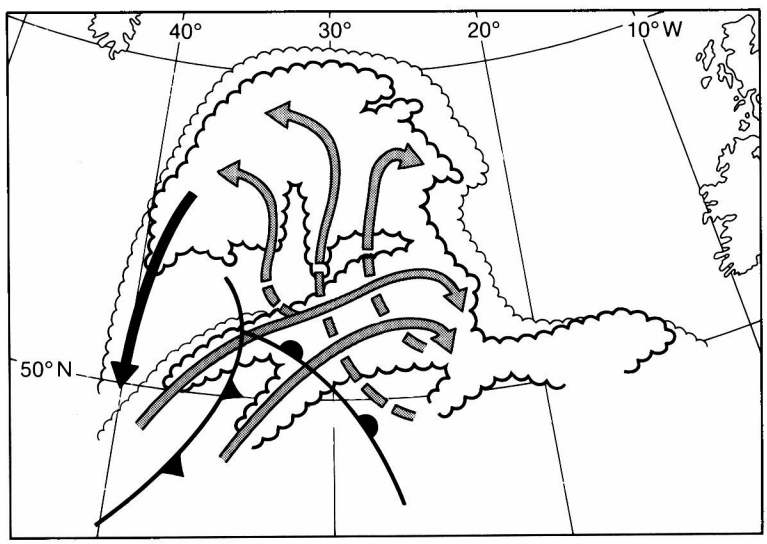

Figure 9. Relative flows within the deepening depression at 0600 GMT on 14 December 1986. The stippled arrows represent 'conveyor belt' motions with ascent occurring within the cloud masses, and the solid arrow represents descent to the rear and near the cloud edge. The bold outline represents thicker cloud while the thinner outline indicates the boundary of more fibrous cloud.

6. Relative motion within the fronts

At midnight on 15 December the position of the surface occlusion was almost vertically beneath the rear edge of its associated cloud mass. Wet-bulb potential temperature (θ_w) is an indicator for defining air mass, and should be conservative for motion within the frontal band. The system relative motions computed for an appropriate θ_w should give an idea of the conveyor belt motions. Just ahead of the surface occlusion are a number of radiosonde stations at points along much of its length. The ascents from each of these stations were plotted and the levels of θ_w of 283 K, 285 K and 288 K were assessed. The winds relative to the front were calculated from the resultant of the winds at these levels and the velocity of the front. In each case, frontal velocity was taken from that part of the front nearest the station.

Fig. 10 shows the flow of air within the system on the 283 K, 285 K and 288 K isentropic surfaces. The warm, moist air ascends quite steeply from 700 mb at Valentia, initially parallel to the front. The flow diverges from the front further north and at Thorshavn it turns away towards the east at 330 mb. The cooler air initially moves in towards the front, particularly at the lower level, with the 285 K surface ascending at a steeper angle than the 283 K surface. The flow becomes parallel to the front over Iceland and diverges from it over Greenland.

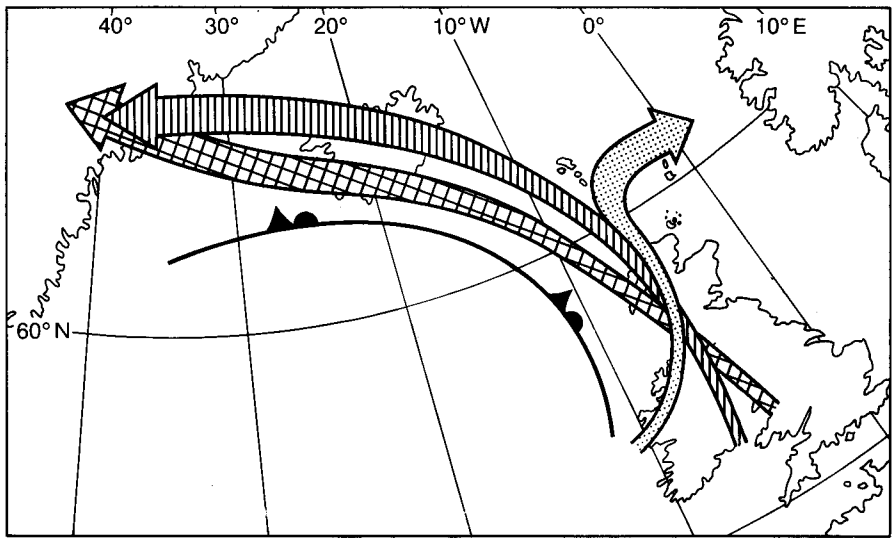

Figure 10 Schematic representation of the flow on the 283 K (hatched arrow), 285 K (shaded arrow) and 288 K (stippled arrow) isentropic surfaces ahead of the occluded front as it approached the British Isles at 0000 GMT on 15 December 1986.

In an attempt to verify these motions within the frontal system as it crossed the British Isles, a movie-loop was made of 31 half-hourly Meteosat images from 1400 GMT on 14 December to 0500 GMT on 15 December. This showed cloud at relatively low levels near to the occlusion moving northwards parallel to it. Cloud at higher levels appeared to move in 'surges', initially parallel to, and slightly ahead of, the cold front and occlusion. The three levels of cloud that can be detected ahead of the cold front in Fig. 5 are probably areas where surges are taking place. One surge pushed well to the north, but later surges made less northward progress and sank away southwards as they reached the forward cloud edge. The dissipation of cirrus and lower-level cumulus ahead of the main frontal cloud showed evidence of marked descent in the downstream ridge. Later in the loop, cloud at higher levels north of the triple point began to become more broken.

7. Conclusions

Enhancement techniques can be used effectively on satellite imagery to accentuate interesting features. They have been used in this case to show how the associated frontal cloud developed and decayed throughout the lifetime of this extraordinary depression. The series of pictures also shows how the intense development rapidly produced large areas of cloud. The depression grew from the convergence of a fast moving wave with an initially small low. The cloud masses associated with the two systems always remained separate and developed equally rapidly, the more northerly becoming part of the occlusion. The area between the two cloud masses was of interest in that it showed the structure of lower-level cloud. The higher-level cloud associated with the cold front and triple point moved well ahead of the corresponding surface features, indicating that most precipitation might be expected near

the warm front. This is confirmed by the surface observations. As the depression matured, cold air became increasingly drawn in to the system. Maximum development coincided with cold air reaching the vortex. Once the depression had begun to fill, cloud soon became broken and less organized, even though the surface pressure remained relatively low.

The existence of conveyor belts within the system, which had been inferred from synoptic data, was verified to some extent, particularly where lower-level cloud was visible. The 'surge-like' motions within the frontal cloud evident from the Meteosat movie-loop were of particular interest.

References

Browning, K.A.	1985	Conceptual models of precipitation systems. *Meteorol Mag*, **114**, 293–319.
Burt, S.D.	1987	A new North Atlantic low pressure record. *Weather*, **42**, 53–56.
Harrold, T.W.	1973	Mechanisms influencing the distribution of precipitation within baroclinic disturbances. *Q J R Meteorol Soc*, **99**, 232–251.
Schwalb, A.	1978	The TIROS-N/NOAA A–G satellite series. Washington, NOAA, Tech. Memo. No. NESS 95.
Turner, J., Eyre, J.R., Jerrett, D. and McCallum, E.	1985	The HERMES system. *Meteorol Mag*, **114**, 161–173.

551.508.824:551.585.7(412)

Weather observations on Cairn Gorm summit 1979–86

J.S. Barton

Department of Physics, Heriot-Watt University, Edinburgh

Summary

An automatic weather station specifically designed for a mountain environment is described, together with a short account of its operation, data dissemination and observations of temperature and wind speed on the summit of Cairn Gorm, Scotland, for the period 1979–86.

1. Introduction

Weather observations on high ground in Britain have never been plentiful, because of the difficulties imposed by a severe climate and the lack of a strong commercial stimulus, in contrast to the development of marine or aviation meteorology. Taylor (1976) reviewing upland climate data wrote of '... the extreme paucity of primary information on our upland climates which necessitates the substitution of crude and unavoidable upslope extrapolation from lowland stations'. There is a limited but growing demand for data on British mountain climates relating to hydrology, forestry, design and siting of wind turbines and communication aerials, skiing developments and forecasting for the large number of recreational hill-walkers and imate data wrote of '... the extreme paucity of primary information on our upland climates which necessitates the substitution of crude and unavoidable upslope extrapolation from lowland stations'. There is a limited but growclimbers throughout the year. For example, Davison (1987) describes the problems of assessing snow-lie in the Scottish Highlands in planning ski developments. This paper gives a short account of a specialized automatic weather station (AWS) situated on an exposed mountain summit, and a brief survey of its observations.

2. Historical background

No survey of mountain weather should omit mention of the manned observatory on Ben Nevis summit (1883–1904), which even now is the largest British observational record of all weather elements in such an environment (Roy 1983). Apart from Ben Nevis, most other sites with significant data are on hill tops carrying radio mast installations such as Lowther Hill and Great Dun Fell (Fig. 1). A few small-scale and necessarily shorter-term studies have been made by enthusiasts such as Baird in the Cairngorms (Baird 1957) and Pedgley in Snowdonia (Pedgley 1974).

In 1971 the deaths from exposure of six young people hill-walking on the Cairngorm plateau led to an examination of improved forecasting for such areas. The outcome of a meeting of the Advisory Committee for Meteorology in Scotland in 1975 was a research proposal by the Heriot-Watt Physics Department, in collaboration with the Institute of Hydrology and the Meteorological Office, to the Natural Environment Research Council for development of an AWS station capable of functioning throughout the year on Cairn Gorm summit. This was a uniquely-favourable site in that, although Britain's fifth highest mountain (1245 m), it already boasted a small stone-built hut with mains power supply, housing radio relay equipment for mountain rescue co-ordination. A skiing development on the northern slopes provided relatively easy access by road and chairlift to within 1 km of the summit.

The problems faced were heavy icing and strong winds in the lengthy winter season which prevented unattended operation of normal instruments. A manned observatory on the Ben Nevis pattern would have been far too costly, while even once-daily visits by staff from the ski area could not guarantee continuity of readings. The Heriot-Watt solution was to place normal instruments inside a heated housing from which they could be automatically deployed to sample the weather. The concept was tested by building a prototype which was installed in March 1976 (Curran *et al.* 1977). The research grant led to construction of a better-engineered Mark 2 version which was mounted on a gantry on the hut roof on 12 March 1977 (Fig. 2). This AWS is still operating without any major design changes. The Institute of Hydrology have developed a separate AWS, continuously exposed and actively de-iced (Strangeways 1985).

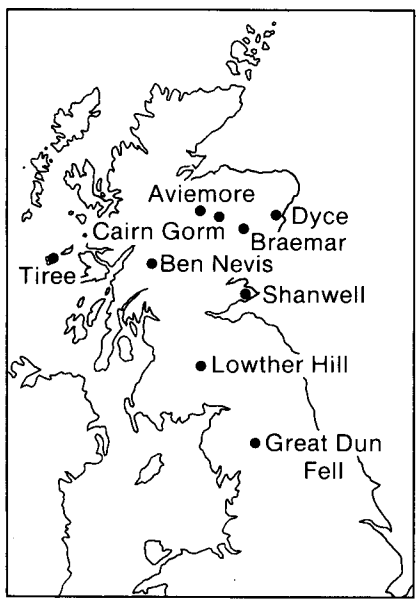

Figure 1. Location of sites mentioned in the text.

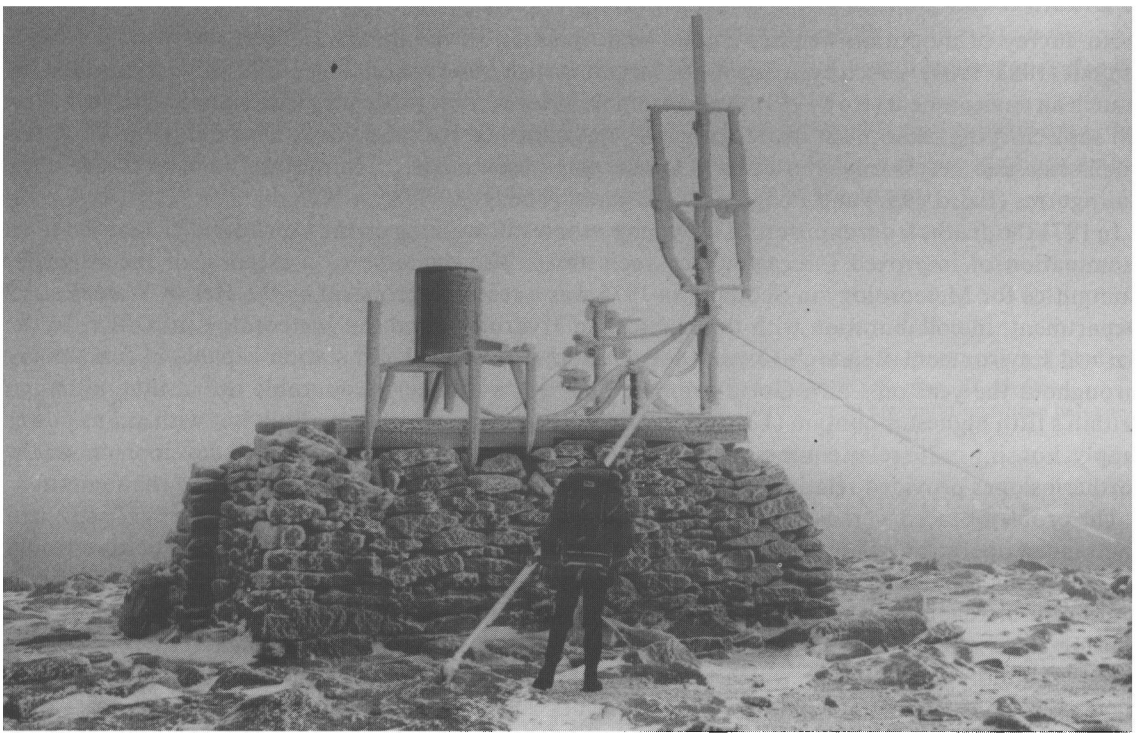

Photograph by courtesy of Heriot-Watt University, Edinburgh

Figure 2. Photograph of Cairn Gorm summit looking south. The AWS is the black cylinder, here shown in the closed position. To the right is a conventional AWS that was temporarily installed for comparison purposes.

3. AWS design

The body of the AWS is cylindrical, 0.63 m in diameter and 0.95 m high, formed from three removable fibreglass panels on an aluminium framework. The sensor platform is normally retracted inside the cylinder and sealed by its lid until the AWS is opened automatically by a 150 W electric motor driving a screw mechanism. The instruments are deployed for 3 minutes every half hour, kept ice-free by thermostatically-controlled heaters (700 W total) inside the housing. After logging the data the AWS closes until the next observation is due. The control and data-logging electronics are within the hut, linked to the AWS by multicore cable.

The instruments are relatively conventional; two dry-bulb platinum-resistance thermometers, a Porton anemometer and wind vane. One thermometer is passively shielded against moisture and radiation, the other is force-ventilated. The 3-cup anemometer is rated to 75 m s^{-1}, with an accuracy of $\pm 2\%$, and is mounted with cups downward on the underside of the lid, being 4 m above the ground when deployed. The wind vane is mounted vertically below the anemometer, reading to an accuracy of $\pm 3°$, smoothed by a 30-second time constant. Data logged every 30 minutes are temperature, 2½-minute mean wind speed and 3-second maximum gust and direction.

It is not possible to use wet-bulb thermometers with any reliability in sub-zero temperatures, while a thin-film humidity sensor has not proved stable enough for long-term operation, possibly due to condensation and thermal cycling in deployment. Precipitation measurement has not been attempted,

partly through difficulty of ensuring sufficient accuracy in a short sampling time, and partly because of the problems of collecting rain or snow in high winds. Further details of the AWS are given by Baker *et al.* (1979) and Barton (1984).

4. AWS operation

Although the fundamental mechanical design has not been changed, some detail improvements have contributed to reliability and ease of maintenance. The station has made more than 146 000 open–close cycles since installation. The AWS was removed to Heriot-Watt for refurbishing from May to July 1982, followed by an intercomparison with standard instruments at Eskdalemuir Observatory from July to August. Only two serious breakdowns have led to prolonged gaps in the data; from August to October 1978 after the AWS was struck by lightning, and from December 1983 to March 1984 caused by mechanical trouble with the screw mechanism.

Routine visits are made at about 6-week intervals to change the logger tape and check calibrations; annual maintenance is performed each summer. Winter (i.e. November to April) brings the hazards of cold, wind and 'white-out' visibility if full snow cover is combined with hill fog and perhaps blowing snow also. The summit path-marker cairns and posts can become rime-covered and invisible, and careful navigation is sometimes required simply to find the AWS. Access becomes impossible in severe winter storms, when conditions on the summits can only be guessed from the AWS observations and by extrapolation from personal experience in uncomfortable but less extreme weather.

5. Data dissemination

The data dissemination has evolved from simple on-site data-logging on cassette to VHF telemetry based on a Meteorological Office system, which is received by several independent base stations (Fig. 3).

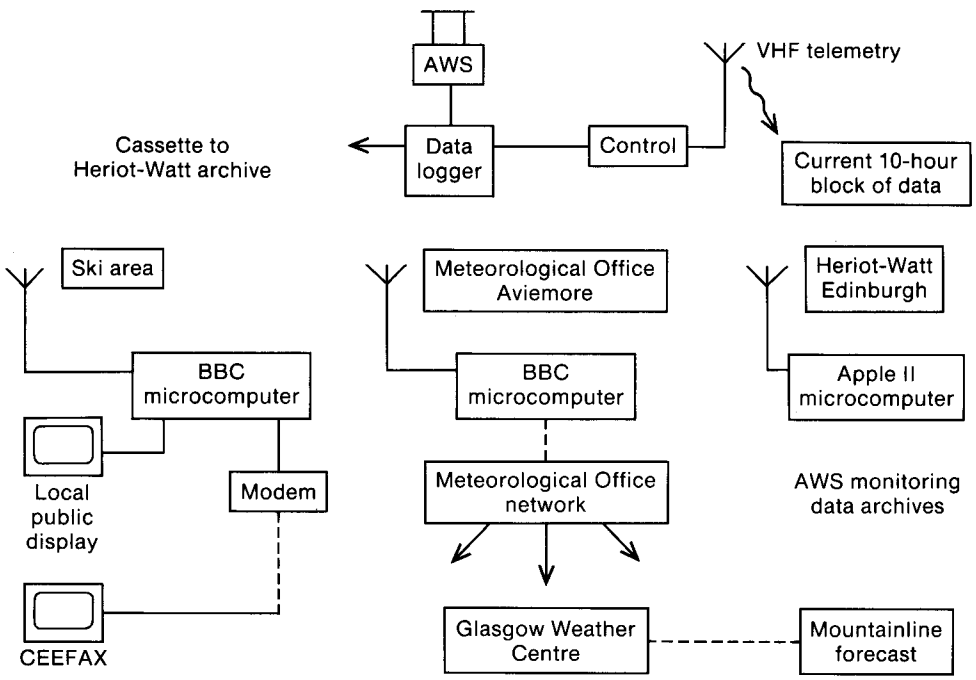

Figure 3. Block diagram of the data dissemination system.

Real-time data transmission is vital for forecasting and important in monitoring the AWS so that faults can be speedily rectified. The Heriot-Watt receiving station uses an Apple II microcomputer while the two more recent stations are based on BBC machines. A local public display at the Cairngorm Ski Area has been supplemented since January 1987 by CEEFAX information pages which include summit observations and a local forecast. Data received at Aviemore Meteorological Office, about 16 km from the summit, are quality checked by the duty observer and telephoned in coded form to Lossiemouth for onward transmission to Bracknell. AWS observations (usually 0400 and 1600 hrs) are included in the Mountainline telephone forecast issued twice daily by Glasgow Weather Centre, which covers popular Scottish mountain areas. Cassette data are quality controlled and archived as daily and monthly summaries at Heriot-Watt University.

6. Brief survey of observations 1979–1986

Data from October 1978 to December 1982 have been archived and analysed by the University of Edinburgh Meteorology Department (Borthwick 1983). No gust observations were made prior to October 1978 and the 1977/78 data have not been analysed in detail. The Edinburgh and Heriot-Watt archives form a data set used as the basis for this survey, covering complete years 1979–86 inclusive.

It should be emphasized that the observations are site-specific, and some caution should be exercised in interpretation and in extrapolation to other mountain areas. An example is the influence of topography on wind speed; summit wind observations may have little relevance to ridge or corrie sites only 1 or 2 km away. Cairn Gorm has a rounded summit, and although there are valleys and cliffs in the surrounding area, the exposure is much more symmetrical than that of Ben Nevis summit, where the proximity of a 550 m cliff strongly affects winds except from the south-east sector.The AWS temperature and wind speed observations 1979–86 for Cairn Gorm are summarized in Tables I and II.

6.1 *Temperature statistics*

The temperature data are based on 48 half-hourly observations reduced to daily and monthly statistics. Data for 1982 are incomplete as the AWS was out of service from mid-May to September, so 1982 has been excluded as being unrepresentative. The overall mean annual temperature (1979–86 excluding 1982) of +0.9 °C can be compared with the Ben Nevis mean (1884–1903) of −0.3 °C (Roy 1983). As Ben Nevis is approximately 100 m higher than Cairn Gorm, on simple lapse rate grounds one might expect the difference in means to be approximately 0.6 °C, i.e. half the observed difference, but the sample is too short to allow firm conclusions to be drawn.

The maximum monthly mean tends to occur in mid to late summer, while the highest individual temperatures are sometimes observed on hot days in May. The minimum month and overall minimum temperature tend to occur closer together in February or March. In cold weather there is a distinction between inversions and relatively uniform lapse-rate conditions. For example, very low minima were observed at valley sites in January 1982 (−26.8 °C at Grantown-on-Spey on the 8th and −27.2 °C at Braemar on the 10th), while the Cairn Gorm minimum was −12.6 °C on the 8th. The author recalls visiting the AWS on 7 and 8 January in conditions of extreme clarity and sunshine above valley-level haze in the inversion layer about 100 m deep.

The lowest summit-temperatures have been observed in easterly winds in polar continental air with a high lapse rate. For example, the lowest minimum of −16.5 °C occurred on 12 January 1987 in south-east winds of 7–15 m s^{-1}. There was no significant diurnal variation, with a maximum of −15.0 °C and a daily mean of −15.9 °C. The Shanwell radiosonde ascent at 1200 GMT gave a lapse rate between 5 m and 1603 m of 9.4 °C km^{-1}, quite close to the dry adiabatic value. Comparison with low-level stations at Dyce (Aberdeen) and Aviemore is interesting since the Dyce temperatures were almost

Table I. *Cairn Gorm summit temperature statistics (°C) 1979–86 inclusive*

Year	1979	1980	1981	1982*	1983	1984	1985	1986	1979–86†
% data	49	74	83	52	90	67	99	85	
Overall maximum	18.6	18.0	16.2	12.0	21.6	18.3	18.0	22.8	22.8
Date	18 June	16 May	12 May	14 May	22 July	22 Aug.	3 June	28 June	28 June 86
Maximum monthly mean	6.2	6.2	6.8	3.1	10.6	9.1	7.2	7.2	10.6
Month	June	Aug.	Aug.	Sept.	July	Aug.	July	June	July 83
Annual mean	−1.0	0.3	1.1	—	1.9	2.9	1.0	−0.2	0.9
Minimum monthly mean	−9.1	−4.6	−4.2	−3.7	−4.3	−5.2	−5.1	−7.6	−9.1
Month	Feb.	Jan.	Dec.	Mar.	Feb.	Mar.	Jan.	Feb.	Feb. 79
Overall minimum	−15.3	−11.4	−11.4	−12.6	−11.7	−9.3	−12.0	−12.0	−15.3‡
Date	14, 15 Feb.	31 Jan. 1 Feb.	22 Mar.	8 Jan.	10 Feb.	31 Mar.	12 Feb.	1 Mar.	14, 15 Feb 79

* AWS overhaul and calibration mid-May to end of August
† Excluding 1982
‡ Lowest minimum −16.5 on 12 Jan. 87

Table II. *Cairn Gorm summit wind observations (m s^{-1}) 1979–86 inclusive*

Year	1979	1980	1981	1982*	1983	1984	1985	1986	1979–86†
% data	47	83	88	51	88	66	98	85	
Annual mean	12.3	12.9	13.4	15.9	13.3	12.6	12.9	14.9	13.3
Maximum monthly mean	15.5	20.2	20.3	17.9	24.5	17.4	16.0	19.1	24.5
Month	Nov.	Dec.	Jan.	Nov.	Jan.	Dec.	Feb.	Nov.	Jan. 83
Maximum daily mean	25.9	30.3	31.4	33.9	37.3	39.8	35.6	34.7	39.8
Direction	SW	W	NW	W	W	SE	SE	S	
Date	4 Dec.	18 Apr.	6 Feb.	19 Nov.	5 Mar.	23 Mar.	9 Feb.	15 Mar.	23 Mar. 84
Maximum 2½-minute mean	39.5	41.1	47.5	45.9	55.6	57.8	46.6	51.4	57.8
Direction	S	W	S	S	NW	SE	SE	S, NW	
Date	12 Dec.	29 Dec.	13 Dec.	26 Oct.	17 Jan.	24 Mar.	8 Feb.	15 Mar., 30 Oct.	24 Mar. 84
Maximum 3-second gust	49.1	56.4	54.0	52.3	65.2	65.1	54.6	76.3	76.3
Direction	SW	W	S	SW	W	SE	W	SE	
Date	4 Dec.	29 Dec.	13 Dec.	12 Feb.	25 Oct.	24 Mar.	31 Jan.	20 Mar.	20 Mar. 86

* AWS overhaul and calibration mid-May to end of August
† Excluding 1982

constant at −5.5 °C throughout the day, while Aviemore showed marked diurnal variation. Winds at Aviemore were lighter, and temperatures ranged from −15.7 °C at 0600 GMT to −6.9 °C at 1400 GMT. This illustrates well the local variations possible between valley and summit.

The lowest minimum on Ben Nevis summit was −17.4 °C on 6 January 1894, following a period of easterly winds. The corresponding observation at Fort William, near sea level, was −5.5 °C giving a lapse rate of 8.9 °C km^{-1}.

Borthwick (1983) has compared AWS monthly mean temperatures with 850 mb temperatures from the Shanwell radiosonde ascents for 1980. Allowing for the height of the 850 mb surface (about 1380–1500 m) by applying an average lapse rate of 6 °C km^{-1}, AWS temperatures are generally within 0.6 °C of the free-air values, but over 1 °C below in February and April. Clearly a more detailed analysis of the full data set would be required to reveal any systematic effects.

6.2 *Wind statistics*

The wind statistics in Table II reflect the exposed nature of the site. The overall annual mean (1979–86, excluding 1982 as unrepresentative) of 13.3 m s^{-1} can be compared with 7.9 m s^{-1} (1961–70 average) for Tiree, an exposed coastal site (Shellard 1976) and with 6.4 m s^{-1} (1895–1904 average) for Ben Nevis summit (Borthwick 1983). This latter figure shows the sheltering effect of the Ben Nevis topography.

Extremes for averaging times ranging from 2½ minutes to 1 month are listed, together with the relevant wind direction to the nearest 45°. Not surprisingly, the strongest winds occur in the autumn and winter months either as westerlies or between south and south-east. Some noteworthy examples of westerly gales occurred on 29 December 1980 (cold front), 17 January 1983 (cold front), 25 October 1983 (warm front) and 30 October 1986 (cold front); the front named being that associated with the strongest winds during the episode. Very strong winds, often in cold air, also occur if fronts are aligned roughly north–south over Britain in a strong south or south-easterly flow. Examples of this situation were observed on 6–7 December 1978, 21 January 1984 (a storm resulting in the exposure deaths of five mountaineers in the area and widespread blockage of roads), 23–24 March 1984 and 15 and 20 March 1986.

The high average and extreme speeds suggest that the mountain's topography may be causing an acceleration of the free atmosphere wind, particularly if stable layers constrict the flow vertically. This possibility is supported by Borthwick (1983) who compared Cairn Gorm and upper-air winds. Using monthly mean winds for 1980, the ratio for Cairn Gorm summit to the Shanwell 850 mb value was 1.21 ±0.13 averaged over 12 months. Further analysis of individual case studies would be of interest in understanding how the atmosphere flows over a mountainous area.

Because the AWS samples only two 2½-minute periods each hour, the gusts recorded are clearly not necessarily the maximum for the hour, as would be obtained from a continuously exposed instrument. The AWS gust is the maximum of 50 contiguous 3-second measurements during the 2½-minute wind-averaging time, therefore the timing of the gust with respect to the 3-second periods is also significant. Overall, the observed ratio of gust to 2½-minute mean speed is approximately 1.25. Gusts over 100 m.p.h. (approximately 45 m s^{-1}) have occurred every winter to date. Not included in Table II is the second highest recorded gust of 66.0 m s^{-1} in a south-easterly gale on 7 December 1978.

The highest gust of 76.3 m s^{-1} was observed at 0049 GMT on 20 March 1986 (mean speed 45.0 m s^{-1}, direction 168°, temperature −5.4 °C) preceded by a gust of 61.0 m s^{-1} half an hour earlier. A deep depression was moving north-east across northern Scotland with an occluded front passing the Cairn Gorm area around 1000 GMT. Winds then veered rapidly to the north-west and increased in the afternoon. Gusts exceeded 45 m s^{-1} from 1119 to 1719 GMT inclusive with a maximum of 67.5 m s^{-1}

(mean speed 49.8 m s^{-1}, direction 306° and temperature −4.5 °C) at 1449 GMT. Winds decreased later in the day as the pressure gradient eased.

7. Conclusions

The Cairn Gorm observations constitute a limited but useful data set relating to climatic conditions of exposed summits in the Scottish Highlands. Comparison with the Ben Nevis observations reveals a broadly similar temperature regime, but a much higher mean wind speed reflecting the different exposures of the two summits. Extreme winds with gusts exceeding 60 m s^{-1} have been observed on several occasions, in agreement with the Ben Nevis observers' estimates.

Data are being used in real time as an aid in the difficult task of forecasting for the mountains in the area, and it is hoped that the AWS will continue operation in order to build up a climatologically significant set of observations of this interestingly severe climate.

Acknowledgements

The author gratefully acknowledges the Meteorology Department of the University of Edinburgh and A.S. Borthwick for permission to use his thesis; Miss M.G. Roy, Edinburgh Meteorological Office for supplying and analysing both contemporary comparison data and Ben Nevis statistics, and A.J. Quinn, Heriot-Watt University, for maintaining the AWS.

References

Baird, P.D. 1957 Weather and snow on Ben Macdui. *Cairngorm Club J.* **17**, 147–149.

Baker, B., Curran, J.C., Harrison, F., Peckham, G.E. and Smith, S.D. 1979 An automatic weather station for operation in severe icing climates. *J Phys E: Sci Instrum*, **12**, 734–738.

Barton, J.S. 1984 Observing mountain weather using an automatic station. *Weather*, **39**, 140–145.

Borthwick, A.S. 1983 Mountain weather in Scotland (thesis). (Unpublished, copy available in University of Edinburgh.)

Curran, J.C., Peckham, G.E., Smith, D., Thom, A.S., McCulloch, J.S.G. and Strangeways, I.C. 1977 Cairngorm Summit automatic weather station. *Weather*, **32**, 60–63.

Davison, R.W. 1987 The supply of snow in the eastern Highlands of Scotland: 1954–5 to 1983–4. *Weather*, **42**, 42–50.

Pedgley, D.E. 1974 Field studies of mountain weather in Snowdonia. *Weather*, **29**, 284–297.

Roy, M.G. 1983 The Ben Nevis meteorological observatory 1883–1904. Part 1. Historical background, methods of observation and published data. *Meteorol Mag*, **112**, 318–329.

Shellard, H.C. 1976 *In* Chandler, T.J. and Gregory, S. (eds); The climate of the British Isles. London, New York, Longman.

Strangeways, I.C. 1985 A cold regions automatic weather station. *J Hydrol*, **79**, 323–332.

Taylor, J.A. 1976 *In* Chandler, T.J. and Gregory, S. (eds); The climate of the British Isles. London, New York, Longman.

551.501.9(458.2):551.5(09):355.48

The Meteorological Office, Valletta, Malta 1942–45

T.A. FitzPatrick

Glasgow*

Summary

An account of activity at Air Headquarters, Malta from October 1942 until May 1945 is given, based entirely on the author's memory of events during that period.

1. October 1942–July 1943

1.1 *The Meteorological Office in Valletta*

I was posted to Air Headquarters (AHQ) Malta from Sullom Voe in the Shetlands in July 1942, and given a Civilian Component commission in the RAF with the rank of Flight-Lieutenant. (At a later date Meteorological Officers were re-commissioned in the RAFVR.) After a short interim posting to Abbotsinch, I eventually reached Malta towards the end of October, along with two other Meteorological Branch officers, Flt Lt J.R. Scott and Flt Lt A.M. Lewis. We travelled out on HMS *Welshman*, a vessel built for laying mines in enemy waters and one of the fastest ships in the Navy. On our outward journey we were held up for about three weeks in Gibraltar while the invasion of North Africa began, and were able to spend a little time at the Meteorological Office there.

The Meteorological Office in Valletta was located in (and later on) the St. John Cavalier, a massive building which was part of the medieval fortifications built by the Knights of Malta during the Great Siege of 1565. It was situated at the highest part of the small peninsula on which Valletta stands, with a commanding view over Malta's two magnificent natural harbours, the Grand Harbour and Sliema Harbour, and over the surrounding sea to north and east. It consisted of a truncated pyramid on a square base, which had served the Knights as a fort, a look-out point and a stable for horses. There was a large internal chamber (see Fig. 1) at the centre of the base which originally had been the stable. A sloping tunnel leading from the entrance at ground level ended in a flight of steps which gave access to the flat top of the building. Here had stood a solid structure built of the distinctive Malta stone, which had been occupied by the Meteorological Office in peace-time. It had had ample space to accommodate forecasting and ancillary meteorological staff, wireless operators, deciphering staff and runners — the latter a necessary element in the wartime situation — and their equipment. However, the office had been severely damaged by enemy action, and at the time of our arrival all its work was being carried out in the tunnel.

If memory serves, the layout there was somewhat as is indicated in Fig. 1; the wireless telegraphy (W/T) section, consisting usually of two or three operators on watch at any time, occupied the first part, seated along the wall of the tunnel one behind the other. Next to them were the 'cipherines' (C) — Maltese girls, to whom the messages received were passed for decoding and then passed on to the meteorological assistants (A), most of whom were Maltese civilians with a few service personnel in addition, who plotted the charts and carried out the observations which of course had to be encoded before being transmitted by W/T. The charts were then taken over to be analysed and drawn up by the duty forecasters (F). Elsewhere in the tunnel, space had to be found for the administrative staff.

*Formerly of the Meteorological Office

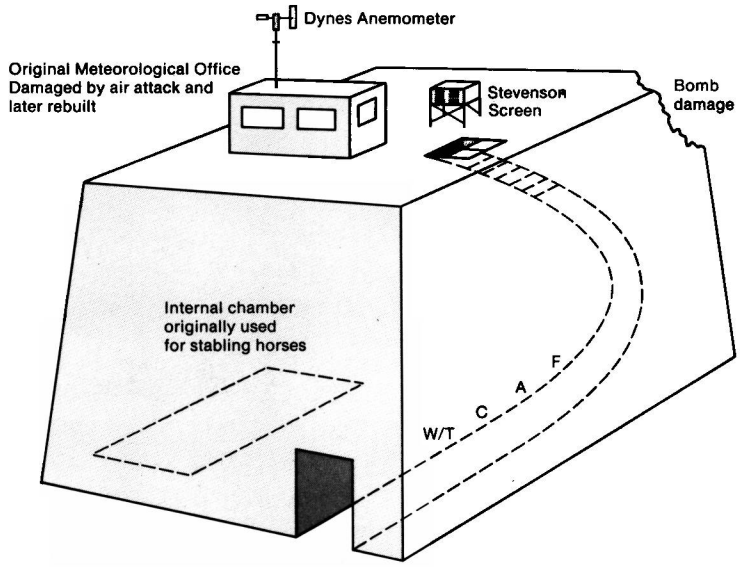

Figure 1. The St. John Cavalier, part of the fortifications of Valletta showing the position of the peacetime meteorological office and the tunnel in which the staff were located following bomb damage. The positions shown are the duty forecaster (F), the meteorological assistant (A), the cipherines (C) and the wireless operators (W/T).

In October 1942 the Senior Meteorological Officer was Sqn Ldr J.H. Brazell, with whom I had worked as a trainee in Invergordon in the spring of 1940, and whom I had met again briefly at Wick. On the staff were Flt Lt McCaffrey and one or two others whose names I cannot now recall, whom we had come to relieve, and Lt W. Eccles, RNVR, the Naval Liaison Officer. I recall also Flt Lt 'Johnny' Johnson, a Canadian officer, who was on the staff with me for a considerable period. Administration was in the hands of Fg Off May and Mr Angelo Ghigo, a local man with considerable length of service, whose prime task was to look after the arrangements for the Maltese personnel. Fg Off Allan Logan (eventually posted to a Mobile Meteorological Unit in the Western Desert) and Fg Off Edward Pyrah were also recent arrivals. Both were posted to the airfield at Luqa, the principal operational base on the island. There were also operational bases at Hal Far (Fleet Air Arm) and Ta'Qali (Fighter Command) and a flying-boat base at Kalafrana at the south end of the island. The Meteorological Office staff in 1943 are shown in Fig. 2.

1.2 *The needs of the RAF, Royal Navy and the Army*

At this time Malta was still in a state of siege. Although victory at Alamein was achieved by about the first week of November 1942, full relief had to wait until the Eighth Army had reached Tripoli, which it did in February 1943. The routine at AHQ Malta was extremely heavy. The Meteorological Office had responsibility for coverage of the central Mediterranean from 5° to 15° E, with no specific limit to the south or to the north, and the area of interest stretched northwards across France to the United Kingdom and southwards into the Western Desert, as well as including all neighbouring parts of the Mediterranean theatre. Weather information had to be supplied to the RAF, Royal Navy and the Army. The demands were enormous.

The needs of the RAF were perhaps self-explanatory; they did include however the broadcast, daily at a fixed-time, of landing conditions at Malta for an aircraft which took off from Gibraltar to run the gauntlet to Malta, and which listened out for this forecast before reaching its point of no return

Figure 2. Some of the Meteorological Office staff, Valletta 1943. Back row — Maltese airmen, W/T operators and meteorological assistants, middle row — Maltese airmen (runners), 5 cipherines, and meteorological assistants and front row (seated left to right) Mr Naudi, Fg Off Rushton, Fg Off May, Flt Lt Johnstone, Flt Lt Scott, Sqn Ldr Brazell, Lt Randall, Flt Lt FitzPatrick, Fg Off Logan, and Mr Ghigo (senior Maltese assistant).

somewhere over Tunisia. A striking force of bombers operated from the island in support of the armies in North Africa, and various transport flights were made to the east and to the west over enemy-occupied territory. When, later, conditions improved as a result of military successes, first in North Africa and the Western Desert and later over Sicily, Italy and Europe generally, weather information had to be provided for flights south and west to North Africa and Gibraltar, east to points in the Middle East, and over occupied France to the United Kingdom, as well as around the central Mediterranean generally. A Photographic Reconnaissance Unit operated from Malta over targets in the Western Desert, Libya, Tripolitania and Tunisia as well as Sicily and southern Italy.

For the Army, the Office issued details of upper-air temperatures and winds for the anti-aircraft batteries, and when the First and Eighth Armies entered our area in North Africa, forecasts of weather conditions in the Western Desert were issued to Army and Air Command. It was rarely possible to check on the accuracy of these, but I believe it to be the case that, on occasion, warnings which AHQ Malta was able to give of rising sand in the desert were of considerable value to RAF and Army units. Co-operation with the Army in Malta was always good. Once the state of supply of ammunition allowed it, an ack-ack (anti-aircraft) battery would, on request, fire smoke shells to burst at a predetermined height, usually 20 000 or 25 000 ft, so that the upper wind could be determined by observation of the movement of the smoke-puffs by theodolite. This gave more accurate results than the nephoscope, and in any case could be used on occasions of cloudless skies, a fairly frequent occurrence, when the nephoscope of course was of no help.

The Navy was interested primarily in the state of sea and visibility throughout the central Mediterranean, without ever divulging the particular operations of submarines or surface craft that might have been making use of the information. The Fleet Air Arm at Hal Far also depended on AHQ Malta for weather information.

1.3 *Observations and forecasts*

All weather observations were received in code by radio. Broadcasts from the United Kingdom, Almaza (Middle East) and Gibraltar formed the basis of the synoptic chart. In addition we listened to broadcasts from enemy-occupied territory in North Africa, mainly Tunisia and Algiers. Within the meteorological staff a remarkable degree of expertise in breaking enemy codes had developed. I can well recall my own astonishment when I arrived there at the speed with which a change in the code-books being used by the enemy was overcome, and wondering if I would ever be able to make any worthwhile contribution to the exercise, but with experience it became remarkably simple.

The forecasters faced problems that were probably unique because of the island situation and the fact that the nearest land areas were in enemy hands. An additional difficulty arose from the shortage of aviation fuel, so that air sorties had to be strictly controlled and the amount of weather information coming from that source, or from sea-borne operations, was limited and irregular. The processing of weather information also raised problems. The observations which we received had first been put into the international weather code, then recoded into a number code, broadcast, received, deciphered (by which stage they had returned to international weather code form) and then plotted. At every stage errors could occur. When reception was poor or broadcasts were being jammed, plotted reports had to be treated with caution. Even with all the information thus collected, the chart usually remained remarkably free of solid up-to-date information over a vast area surrounding the island, extending south into the Western Desert and north, west and east over Sicily, Italy, Spain, France, the Balkans, Greece and the eastern Mediterranean.

In addition to the problem of lack of hard information, the forecaster had to be able to judge the accuracy or otherwise of the information which had passed through so many processes before reaching him. One illustration of this which comes to mind may be of interest. There was an occasion, probably about late September 1943, when the general state of the atmosphere pointed to the likelihood of an outbreak of thunder. The problem was the obvious one of predicting the time it would occur and giving adequate warning. Observations from Tunisia throughout the day recorded clear skies and a light wind; then in the late evening one report, from the Cape Bon area, showed a change in wind direction from south-east to north-west with some increase in strength. Small amounts of upper cloud were also reported. On the strength of this slender, unsupported and possibly erroneous evidence a storm was forecast, which duly arrived at Malta in all its terrifying glory around 0900 hrs the following morning.

The heavy routine at AHQ was not made less onerous by the requirement that the duty Meteorological Officer had to brief the Air Officer Commanding (AOC) at 0800 hrs every morning, as the culmination of his exhausting night watch. At this time the AOC was Air Vice-Marshall Sir Keith Park, who had already made history, not only by his part as strategist in the Battle of Britain, but also by the spectacular success of his first encounter with the enemy in the Mediterranean, when he used the element of surprise in a most dramatic way. Spitfires, not hitherto seen on the island, took off from an aircraft carrier off the Cape Bon Peninsula and carried out a devastating attack 'out of the blue' on enemy bombers engaged in an unopposed raid on Malta, and then landed on the island. Giving the daily weather briefing to the AOC was particularly exacting, not only because of the paucity of information and the difficulties inherent in the island situation, but also because of the incisive questioning from this very lively-minded Air Officer.

2. Major operational events

Of great interest are the major operational events for which weather information had to be supplied. These were the invasion of Sicily in July 1943, and the Yalta Conference in 1945, for which the principal participants on the Allied side, Churchill and Roosevelt, came together in Malta for their joint

preparation, and flew from there to Yalta. Besides these historic events the other onerous responsibilities of the weathermen, which included forecasting for flights over enemy-occupied territory to the United Kingdom as well as operational flights in support of the Army in North Africa, tended to pale into insignificance. The brief accounts which follow are based entirely on memory.

2.1 *Invasion of Sicily*

By June 1943 the German and Italian forces had been driven out of Africa, but had withdrawn only as far as Sicily. Land, sea and air forces congregated at Malta in preparation for the invasion which began on 10 July 1943. Weather information was required for naval forces, which included a vast array of tank landing-craft, and aircraft which included troop carriers, gliders and towing machines as well as fighters and bombers. In my recollection the weather map was remarkably devoid of information from Malta northwards as far as the United Kingdom. There were observations from Gibraltar, from North Africa from west to east, from the neighbouring islands of Linosa, Lampedusa and Pantelleria (I think; but these observations may not have begun till later), but nothing from Sicily, Italy, France or the Balkans. However the general synoptic situation seemed to suggest that a mistral-type situation had been prevailing in the south of France, with the consequent probability of a depression forming in the Gulf of Lions. The difficulty was to time its genesis and predict its intensity and subsequent speed of movement. A depression did in fact develop and move south into the Tyrrhenian Sea, with the result that the invasion had to take place in the teeth of a wind from the north-west of Force 7, to the great discomfort of many who were making the long sea crossing. One helpful factor for them was the fact that because of the wind direction, the sea conditions moderated as the ships approached the Sicilian coast. Some gliders had an unfortunate experience. Insufficient attention had been paid to the information given about the strength of adverse upper winds above 10 000 ft and some were released too soon and failed to reach the Sicilian coast.

Sicily was soon taken, and thereafter the position in Malta markedly improved. In due time it became possible to send personnel to Sicily for leave, to the rest camps which had been established on Mount Etna and at Taormina. Aerial activity from Malta however continued at an intense level, with increasing numbers of transport and other aircraft flying between the central Mediterranean, the Middle East and the United Kingdom.

2.2 *The Yalta Conference*

This historic event took place in February 1945. For some weeks before, activity at the Meteorological Office at AHQ had increased to a level of intensity which had never previously been reached. Sqn Ldr (now Wing-Commander) Brazell had been posted to Iraq, without replacement. To help meet the increased work-load, and to provide someone with experience of conditions and provision of information in the Black Sea area, Sqn Ldr Chambers was posted temporarily to Malta from Almaza. This addition to the staff, welcome as it was, scarcely stood comparison with the corps of US meteorologists, consisting as it did of a Colonel, two Majors and sundry other junior officers and other ranks, who arrived to oversee the American involvement.

A major problem was the collecting, deciphering and decoding of Russian weather broadcasts from the Black Sea area. The amount of work for the W/T operators more than doubled, and to help out the hard-pressed ciphering staff everyone had to lend a hand. In my recollection, a period of several weeks — perhaps three to four — went past, during which this effort had to be made round the clock, and the weather scanned for a possible trip to Yalta, with particular attention to reasonable landing conditions at Yalta as well as safety *en route*. At this time of the year snow was still liable to occur in the Yalta area, with consequent high risks to aircraft at the limit of their endurance. At the same time the routine work

greatly expanded because of the increased coming and going from the United Kingdom by high-ranking personnel.

When Churchill and Roosevelt eventually set off on a more than normally hazardous journey, AHQ Malta had to co-operate in the provision of weather information for the flights.

The aircraft carrying the principal parties would have a point of no return somewhere in the eastern Mediterranean. To provide fighter protection as far as this was possible, the route would be overflown by a number of Mosquitoes, some flying from Naples and landing at Almaza, others moving in the reverse direction. A Sunderland seaplane would fly the route behind the main body to be ready to pick up survivors from any machine that might be forced into the sea from whatever cause. For all of these, AHQ Malta had to co-operate in the provision of flight forecasts and landing forecasts, and assist in the briefing of aircrew. Needless to say, the responsibilities were shared with the US staff. In all, it was an exciting, exhausting and interesting exercise in international co-operation.

3. Some general points

For forecasters whose practical experience had been gained in higher latitudes open to oceanic influence, transition to the Mediterranean area demanded considerable intellectual adjustment. Because of the land-locked nature of the Mediterranean basin, the high relief of much of its coastal zones and the influence of the vast land mass of Africa and the Sahara, the weather tends to develop in ways not readily described in the clear-cut terms of frontal analysis that work well over the sea in higher latitudes. Phenomena of particular interest to the wartime meteorologist included rising sand and sandstorms in the Western Desert associated with atmospheric instability and intense surface heating, violent thunderstorms, poor visibility, low stratus and sea fog over vast sea areas when all available observations (over land) reported clear skies and excellent visibility, conditions of exceptional visibility (e.g. when the summit of Mount Etna could be seen from Valletta) and violent turbulence at low levels in cloudless conditions. On one such occasion aircraft on escort duty could not maintain station at 2000 ft, although there was no cloud in the sky, but found smooth flying conditions at a mere 4000 ft.

It has to be remembered that, at the time to which these notes refer, aircraft were propellor-driven and limited in range and operational height. Flights made from Malta over occupied France to the United Kingdom frequently had to operate in conditions when icing constituted a high risk. Navigational aids were at an early stage of development and upper-air data limited. When the siege conditions lifted, Malta began its own meteorological flight — a vertical ascent by a Hurricane fighter. Attempts were made to locate thunderstorms over the sea using W/T direction-finding techniques, and to gain information about upper winds by tracking, in the same way, pilot balloons covered with tin foil.

4. Conclusion

I was posted back to the United Kingdom shortly after VE Day, to HQ 18 Group at Pitreavie. It was then expected by many that Transport Command would soon be making big demands on meteorological personnel, but all such speculations were brought to a close by the sudden and horrific ending of the conflict in the Pacific.

Correction

Meteorological Magazine, September 1987, p. 279. The correct title of the article by D. Offiler is 'Wind measurements from the European remote-sensing satellite, ERS-1'.

Satellite photograph — 25 August 1987 at 0400 GMT

This NOAA-9 infra-red image was taken during a period when heavy rainfall and severe thunderstorms affected large areas of western and central Europe. Most apparent is the large comma-shape in the cold-cloud top. This resulted from the merging of cloud bands associated with a cold-front wave (Low E) which had developed ahead of a sharp upper trough, and bands generated chiefly through positive vorticity advection (PVA) closer to the axis of the upper trough (located near 4° E over central France at 0400 GMT). Within the cold-frontal band, in the comma tail, a large shield of anvil cirrus resulting from the combined outflows from numerous cumulonimbus cells covers north-east Italy and Alpine regions of Switzerland and Austria. Flash-floods from these storms caused extensive damage and loss of life. Developing cells can also be seen over central Italy. Within other parts of the comma, especially towards the head, deep convection on a smaller scale can be identified, generated within bands extending across the North Sea, with the resulting anvils shearing northwards in the strong flow aloft. Some other features of interest in the image include the bands of dense cirrus within a region of strong wind shear over central Britain and the circulation associated with an old tropical storm (Low A) situated near 46° N, 17° W.

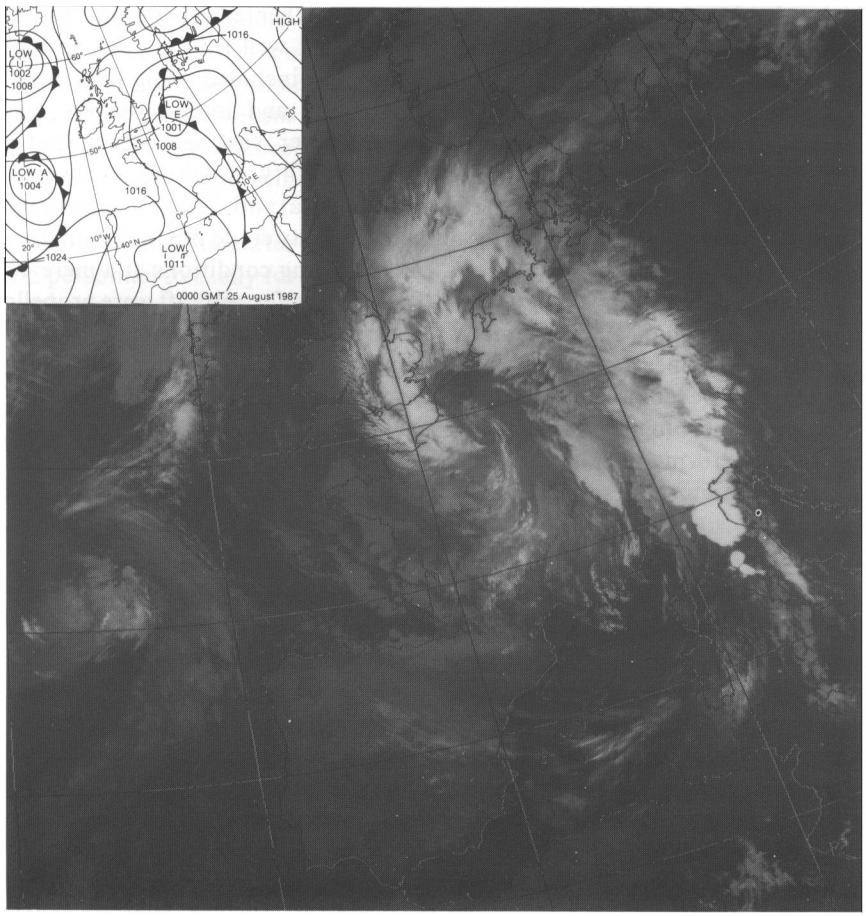

Photograph by courtesy of University of Dundee

Meteorological Magazine

GUIDE TO AUTHORS

Content

Articles on all aspects of meteorology are welcomed, particularly those which describe the results of research in applied meteorology or the development of practical forecasting techniques.

Preparation and submission of articles

Articles for publication and all other communications for the Editor should be addressed to the Director-General, Meteorological Office, London Road, Bracknell, Berkshire RG12 2SZ and marked 'For *Meteorological Magazine*'.

Articles, which must be in English, should be typed, double-spaced with wide margins, on one side only of A4-size paper. Tables, references and figure captions should be typed separately.

Spelling should conform to the preferred spelling in the *Concise Oxford Dictionary*.

References should be made using the Harvard system (author, date) and full details should be given at the end of the text. If a document referred to is unpublished, details must be given of the library where it may be seen. Documents which are not available to enquirers must not be referred to.

Tables should be numbered using roman numerals and provided with headings. We consider vertical and horizontal rules to be unnecessary in a well-designed table; spaces should be used instead.

Mathematical notation should be written with extreme care. Particular care should be taken to differentiate between Greek letters and Roman letters for which they could be mistaken. Double subscripts and superscripts should be avoided, as they are difficult to typeset and difficult to read. Keep notation as simple as possible; this makes typesetting quicker and therefore cheaper, and reduces the possibility of error. Further guidance is given in BS1991: Part 1: 1976 and *Quantities, Units and Symbols* published by the Royal Society.

Illustrations

Diagrams must be supplied either drawn to professional standards or drawn clearly, preferably in ink. They should be about 1½ to 3 times the final printed size and should not contain any unnecessary or irrelevant details. Any symbols and lettering must be large enough to remain legible after reduction. Explanatory text should not appear on the diagram itself but in the caption. Captions should be typed on a separate sheet of paper and should, as far as possible, explain the meanings of the diagrams without the reader having to refer to the text.

Sharp monochrome photographs on glossy paper are preferred: colour prints are acceptable but the use of colour within the magazine is at the Editor's discretion. In either case contrast should be sufficient to ensure satisfactory reproduction.

Units

SI units, or units approved by WMO, should be used.

Copyright

Authors wishing to retain copyright for themselves or for their sponsors should inform the Editor when they submit contributions which will otherwise become UK Crown copyright by right of first publication.

It is the responsibility of authors to obtain clearance for any copyright material they wish to use before submitting it for publication.

Free copies

Three free copies of the magazine are provided for authors of articles published in it. Separate offprints for each article are not provided.

Meteorological Magazine

November 1987

Editor: R.W. Riddaway
Editorial Board: T. Davies, W.H. Moores, P.R.S. Salter, P.G. Wickham

Vol. 116
No. 1384

CONTENTS

Page

Observations of the structure of a deep fog R. Brown 329

The development of an extraordinary depression — a satellite perspective J.N. Ricketts 339

Weather observations on Cairn Gorm summit 1979–86 J.S. Barton 346

The Meteorological Office, Valletta, Malta 1942–45 T.A. FitzPatrick 354

Correction 359

Satellite Photograph — 25 August 1987 at 0400 GMT 360

Contributions: it is requested that all communications to the Editor and books for review be addressed to the Director-General, Meteorological Office, London Road, Bracknell, Berkshire RG12 2SZ, and marked 'For *Meteorological Magazine*'. Contributors are asked to comply with the guidelines given in the *Guide to authors* which appears on the inside back cover. The responsibility for facts and opinions expressed in the signed articles and letters published in *Meteorological Magazine* rests with their respective authors. Authors wishing to retain copyright for themselves or for their sponsors should inform the Editor when submitting contributions which will otherwise become UK Crown copyright by right of first publication.

Subscriptions: Annual subscription £27.00 including postage; individual copies £2.30 including postage. Applications for postal subscriptions should be made to HMSO, PO Box 276, London SW8 5DT; subscription enquiries 01–211 8667.

Back numbers: Full-size reprints of Vols 1–75 (1866–1940) are available from Johnson Reprint Co. Ltd, 24–28 Oval Road, London NW1 7DX. Complete volumes of *Meteorological Magazine* commencing with volume 54 are available on microfilm from University Microfilms International, 18 Bedford Row, London WC1R 4EJ. Information on microfiche issues is available from Kraus Microfiche, Rte 100, Milwood, NY 10546, USA.

ISBN 0 11 727975 7

ISSN 0026–1149

© Crown copyright 1987

Printed in the United Kingdom by Her Majesty's Stationery Office
Dd 0240021 10/87 C15 93379/1 (40711)